Optimization of Batch Polymerization Processes—Narrowing the MWD. I. Model Simulation

BRIAN M. LOUIE and DAVID S. SOONG, *Department of Chemical Engineering, University of California, Berkeley, California 94720*

Synopsis

Several control strategies for the free-radical polymerization of methyl methacrylate are analyzed with a detailed constitutive model incorporating the gel and glass effects. Optimal temperature history, photoinitiation intensity variation, and programmed monomer and solvent additions, employed alone and in combination, represent cases simulated by this model. Solvent addition is selected for further experimental studies, due to some attractive features. The product molecular weight distribution is narrowed, while the molecular weight averages are maintained high. Model predictions of the solvent injection history exhibit a strong sensitivity to the constitutive equations for describing the gel and glass effects.

INTRODUCTION

The mechanical properties of a polymer are related to its molecular weight (MW) and molecular weight distribution (MWD). Martin et al.[1,2] found thermal properties, stress–strain properties, impact resistance, strength, and hardness all improved with narrowing MWD. For a free-radical mechanism with termination by disproportionation, the minimum polydispersity is 2. However, due to concentration and thermal drift, dead-ending, gel effect, etc., this theoretical limit is seldom obtained. Since post-synthesis modification such as preparative GPC is expensive and solvent nonsolvent fractionation techniques are slow and tedious, it is highly desirable to control the MW and MWD during the polymerization process.

In this paper, we will discuss several alternatives to optimize the product characteristics, i.e., the MW averages and MWD. The evolution of process temperatures, initiator decomposition history, and programmed solvent addition are some control strategies examined by modeling and experimentation.

The primary objective of batch process optimization is to achieve a high conversion and produce the desired MW with a narrow MWD. Process time per batch should also be minimized to allow for higher productivity when possible. If a diluent (such as water or solvent) is added, its use must be minimized. This reduces the quantity of material that must be separated and recycled to the reactor. In addition, optimal policies must not be too complex as sudden process changes are difficult to implement. Simple control schemes should be favored over complex ones.

To meet the above requirements, the optimization problem is commonly divided into two categories: minimizing the batch time and narrowing the MWD. In formulating the minimum end time problem, only the final conversion and cumulative average chain length are specified. This leaves the

Journal of Applied Polymer Science, Vol. 30, 3707–3749 (1985)
 CCC 0021-8995/85/093707-43$04.00

MWD uncontrolled. In narrowing the MWD, only polydispersity (PD) is specified (and MW may drift). However, for a well-optimized process, both batch time and PD are important. Unfortunately, obtaining either objective often does not insure the other.[3] Optimum batch policies are then determined using temperature, initiator, monomer, or solvent as control variables.

LITERATURE REVIEW

Numerous works exist for the optimization and control of batch and semibatch reactors with exothermic, first order kinetics. Aris,[4] Hill,[5] and Froment and Bischoff[6] have reviewed the optimal operational policies and control strategies of these reactors.

For free-radical polymerization, work has mainly been on model systems (mainly styrene) with streamlined kinetics, ignoring the glass and gel effects and volume contraction to simplify the mathematics. Optimum policies have little in common and only some experimental validation has been done. Here, review of the optimum batch policies will be done in two parts. Those that minimize PD are examined first. A review of the minimum end-time problem then follows.

Hoffman, Schreiber, and Rosen[7] did some of the earliest work on narrowing the MWD. They reasoned that since monomer and initiator were consumed at different rates, the degree of polymerization (DP, or the number of monomer units in the instantaneous MW) would vary considerably and broaden the MWD. To minimize this drift, they obtained analytical solutions of the kinetic equations to maintain DP constant. Under isothermal conditions, the optimum initiator feed rate drops off with increasing conversion. Optimum monomer addition equations were also developed. They did not include the gel effect, but accounted for volume expansion due to the added feed and volume contraction due to polymerization. Termination was by disproportionation and chain transfer was ignored.

Tadmor and Biesenberger[8] proposed that the narrowest MWD results when the probability of propagation could be made constant. Tadmor and Biesenberger[9] also showed that the maximum effect of thermal drift on the MWD is much greater than that of residence time distribution (RTD) and micromixing. This is supported by Denbigh,[10] who found that the RTD in continuous reactors has little effect on the MWD since the average residence time is much longer than the average lifetime of a growing chain. The QSSA was used to derive rate expressions, and termination was by combination. The gel effect was also ignored.

Nishimura and Yokoyama[11] used the calculus of variations to minimize the variance of the MWD. Their optimum temperature policy kept DP constant, and this was shown to be identical to the minimum PD policy. Concentration drift was eliminated by holding all reactant concentration ratios constant. Chain transfer, gel effect, and volume contraction were all ignored. The QSSA was again used to derive rate expressions.

Hicks, Mohan, and Ray[12] studied the optimum start-up problem for a CSTR and the minimum MWD problem for batch reactors. Their optimum policy also aimed to maintain DP constant. However, they concluded that imperfect mixing effects appeared to be more important than any improve-

ments gained through optimization of perfect mixing models. This is in direct contradiction with the aforementioned findings of Tadmor and Biesenberger.[8] No experimental data were provided to support this claim. The gel effect was ignored, but chain transfer was included.

Osakada and Fan[3] computed the near-optimum temperature and initiator feed profiles for a semibatch reactor using weighted time-integral objective functions. A Simplex search was performed to determine the coefficients of the third-order polynomial, which best approximates the optimum profile. However, they reasoned that PD was not a good criterion for specifying the MWD (since PD changes with DP for the same width of the MWD) and investigated both constant DP and PD policies. For a constant PD, the optimum temperature policy is an isothermal profile, while the optimum initiator policy calls for an increasing quantity of initiator to be added with time. For a constant DP, the near optimum temperature and initiation profiles generally decrease with time first and then increase near the end. They also found that the MWD was not necessarily narrowed when DP was controlled (contrary to Nishimura and Yokoyama[11]). The gel effect and volume contraction were not considered, but chain transfer was included. No experimental verification of the results was provided.

Sachs, Lee, and Biesenberger[13] investigated the effect of temperature on minimizing and maximizing PD using Pontryagin's maximum principle. Their optimum policy also appeared to minimize PD by minimizing changes in the instantaneous MWD caused by declining monomer and initiator concentrations. The maximum PD occurs when there is a sharp step change in temperature. Nonisothermal polymerizations produce PDs somewhere between the minimum and maximum PD. Numerical simulations were compared with experimental results for styrene polymerization. Chain transfer was neglected, and constant density was assumed throughout the reaction. The gel effect was modeled as a polynomial function of the conversion (since viscosity increases exponentially with the quantity of polymer present).

One of the first minimum batch-time problems was solved by King and Skaates,[14] who investigated the on–off heating control of a batch bulk reactor. They wanted to polymerize MMA to 10% conversion as quickly as possible by switching from full heating to full cooling in an external jacket during the batch. At high initiator concentrations, full heating was found optimal, while, at low concentrations, the optimal policy called for a single switch from heating to cooling. Termination by combination was assumed, an empirical gel effect was used, and the viscosity variation with temperature was ignored. No experiments were performed.

Yoshimoto et al.[15,16] studied the optimum time problem for the thermal polymerization of styrene in a batch reactor. The maximum principle was used with temperature constraints. Their optimum policy gradually raised the temperature until the upper constraint was reached. The kinetic chain length decreases with temperature until the desired MW is reached. Faster conversions may be attained at higher temperatures, but at the expense of producing shorter chains. Volume contraction and the gel effect were neglected. Chain transfer was included and the QSSA used to simplify rate expressions. No experiments were performed.

Wu, Denton, and Laurence[17] reexamined the minimum end-time problem for the thermal polymerization of styrene. Inclusion of the gel effect and volume contraction complicated the mathematics, but offered significant improvements in the kinetic model. Results similar to Yoshimoto et al.[16] were obtained. They found excellent agreement between theory and experiments when some of the optimum policies were tested.

Sachs, Lee, and Biesenberger[18] also solved the minimum batch time problem by using the maximum principle. They found that the optimum temperature and initiator addition policies strived to keep the rate of initiator decomposition constant. Inclusion of the gel effect shifted the optimal policies to higher temperatures than if the gel effect had been absent. They also found that dead-ended polymerizations could lead to significantly shorter end-time policies for single initiators loadings. Constant density and QSSA were again used to derive rate expressions, and an empirical gel effect model was used. No experiments were performed.

In a series of papers, Chen et al.[19,20] reinvestigated the minimum end-time policies for continuous addition and one-shot initiator schemes. Results similar to Sachs et al.[18] were obtained for continuous addition policies. However, for single initiator loadings, they noted that there is a unique optimum loading for each desired MW. The "best" isothermal policy was determined with the use of Lagrange multipliers, while the maximum principle was needed to find the optimal nonisothermal policy. The optimum policy was not necessarily better than the isothermal policy if the optimum initiator concentration was not employed simultaneously. Both policies used dead-ending to shorten reaction times. Chain transfer, gel effect, and constant density were incorporated. The QSSA was used to derive rate equations. Good agreement was found between the experimental and theoretical conversion and molecular weights.

From this brief review, three important conclusions can be reached. First, the minimum end time problem apparently is solved by controlled dead-ending. Second, the minimum PD policy attempts to eliminate any drift in the instantaneous MWD. And last, the optimum operating policy (for both optimizations) appears to be highly dependent on the model equations used. Since only model systems have been studied, the results, to date, are inapplicable to more complex or real systems.

This study differs from previous studies in that it employs realistic kinetic models for MMA polymerization instead of generalized model equations. In particular, models for the gel and glass effects derived from free-volume diffusion theory will be used since termination and propagation are both bimolecular diffusion-controlled processes. Most previous investigations have only used ad hoc empirical models. Chain transfer, volume contraction, thermal runaway, and other effects will also be investigated to determine their influence, if any, on the optimum minimum PD policy.

MODEL STUDIES

Several numerical approaches can be used to find the optimal batch operating history. Most of the these techniques are reviewed by Denn.[21] Dynamic programming methods, gradient search techniques, and the max-

imum principle have been used successfully by others because of the simplifications to the kinetics involved. In this work, numerical solutions are required, however, as a result of the highly nonlinear behavior of the rate constants.

At the expense of a great deal more computational work, weighted time-integral objective functions were used in this study. A number of different functions can be devised depending on the final objective. For example, the minimum end time problem can be stated as

$$\min F = w_1(t_b) + w_2(\overline{M}_n - \overline{M}_n^*)^2 + w_3(x - x^*)^2 \tag{1}$$

where w_1, w_2, and w_3 are weighting constants, x^* and $\overline{M}_n^*$ are the desired conversion and number average MW, and t_b is the batch time. If reaction productivity must be optimized, a constant rate objective function may be employed. The objective function would then be

$$\min F = (R_p - R_p^*)^2 \tag{2}$$

where R_p^* is the desired reaction rate. However, since the physical properties of a structural polymer are related to its MW and MWD, the objective function most often chosen in this work is

$$\min F = w_1(\overline{M}_n - \overline{M}_n^*)^2 + w_2(\mathrm{PD} - \mathrm{PD}^*)^2 \tag{3}$$

where PD* is the desired polydispersity. Evaluation of eq. (3) can be further simplified to

$$\min F = \int_0^{t_b} (\mathrm{PD} - \mathrm{PD}^*)^2 \, dt \tag{4}$$

when $w_2 > w_1$ and the instantaneous MWD is centered around the desired MW. Consistent with views expressed in the literature, we believe the MWD will be narrowed if the instantaneous PD is maintained at the minimum value throughout the polymerization, i.e., the cumulative PD is minimized up to any given conversion.

Our approach differs from Osakada and Fan[3] in that the control variable is not fitted with a polynomial. Instead, the full set of kinetic rate expressions is integrated stepwise, and the polydispersity computed. A pattern search (using computed values only) adjusts the control variable and reintegrates the step until the objective function is minimized. In this study, monomer concentration, temperature, rate of initiation, and solvent addition rate will be taken as the control variables. Process constraints (such as the ceiling temperature or maximum flow rates) can be easily incorporated into the optimization as limits on the pattern search. Use of a modified Gear's method for the integration of the nonlinear ODEs reduces the number of evaluations. Results are step-size-dependent, but relatively large steps can be taken when PD does not change rapidly. Smaller steps are required when faster reaction rates are encountered.

The step-by-step nature of the integration process requires the initial conditions be part of the optimal path. This allows the desired PD to be set by the instantaneous MWD (PD = 2), independent of process conditions. The instantaneous MWD is then centered around the desired MW throughout the reaction. The locus of all conversion–time histories for a desired MW with the minimum PD strategy is obtained from the optimization-integration of eq. (4). Shorter reaction times to a given conversion and molecular weight may exist, but the MWD will always be broader than the minimum PD, due to thermal and concentration drifts.

The optimization method, while computationally inefficient, is considerably more flexible than other traditional methods. Realistic kinetic models may be used to represent polymerization systems at high conversions. Chain transfer, volume contraction and volume expansion, and the glass and gel effects may all be properly incorporated. And once programmed, the objective and control variable may be conveniently changed.

The mathematical framework of optimum policies for the control of the molecular weight distribution is now developed. Optimal initiation, temperature, monomer, and solvent addition histories for a semibatch reactor producing PMMA are determined from the step-by-step integration of the rate equations. These equations are developed below. Since poor heat transfer conditions can be expected in a large scale, commercial polymerizer, nonisothermal as well as isothermal analyses have been performed on the optimum policies. Particular attention will be paid to molecular weight and polydispersity behavior.

Methyl methacrylate is commonly polymerized by a free-radical, chain addition mechanism. This process consists of three steps: initiation, propagation, and termination. Free radicals are formed by the thermal fragmentation of initiators. Once formed, these radicals propagate by reacting with surrounding monomers to form long chains. The reaction terminates when two radicals react with one another to yield the final polymer. Chain transfer can also occur when growing radicals react with solvent or monomer molecules to produce short chains. These reactions must also be considered for accurate molecular weight predictions. Table I summarizes the basic free-radical polymerization mechanism.

From the above described kinetic scheme, an infinite number of species mass balances will be needed to model the reaction. To make this problem tractable, the following simplifications are made.

1. Since the chain length of free-radical polymers is long, monomer consumption by primary radicals ($P_1 \cdot$) and by chain transfer reactions can be ignored.

2. The quasi-steady state approximation (QSSA) is applied to primary radicals with all other species balance equations remaining in differential form. (This is more accurate than strictly applying the QSSA to all the radicals as Chiu et al.[22] has shown that the QSSA breaks down at high conversions.)

3. To reduce the infinite number of radical species balance equations, moments of the molecular weight distribution can be used. Moments are defined

$$\lambda_k = \sum_{n=1}^{\infty} n^k[P_n] \quad \text{and} \quad \mu_k = \sum_{n=1}^{\infty} n^k[D_n] \tag{5}$$

TABLE I
Free-Radical Kinetics of Methyl Methacrylate Polymerization[a]

Initiation	$I \xrightarrow{k_d} 2\,R\cdot + G\uparrow$,	$R_d = k_d[I]$
	$R\cdot + M \xrightarrow{k_i} P_1^\cdot$	$R_i = k_i[R\cdot][M]$
	$2\,R\cdot \xrightarrow{k_{ti}} I'\cdot$	$R_{ti} = k_{ti}[R\cdot]^2$
Propagation	$P_n\cdot + M \xrightarrow{k_p} P_{n+1}^\cdot$	$R_p = k_p[P_n^\cdot][M]$
Chain transfer reactions		
With Monomer	$P_n^\cdot + M \xrightarrow{k_f} P_1^\cdot + D_n$	$R_f = k_f[M][P_n^\cdot]$
With Solvent	$P_n^\cdot + S \xrightarrow{k_s} D_n + S\cdot$	$R_s = k_s[S][P_n^\cdot]$
	$S\cdot + M \longrightarrow S + P_1^\cdot$	
Termination	$P_n^\cdot + P_m^\cdot \xrightarrow[\text{(combination)}]{k_{tc}} D_{n+m}$	$R_{tc} = k_{tc}[P_n^\cdot][P_m^\cdot]$
	$P_n^\cdot + P_m^\cdot \xrightarrow[\text{(disproportionation)}]{k_{td}} D_n + D_m$	$R_{td} = k_{td}[P_n^\cdot][P_m^\cdot]$

[a] Symbols: I = initiator (AIBN), R· = primary radical, I′ = recombined initiator fragments, G = gas molecule (nitrogen), M = monomer (MMA), $P_n\cdot$ = live radical of length n, D_n = dead polymer of length r, S· = solvent transfer radical, k_d = initiator decomposition rate constant, k_i = chain initiation rate constant, k_{ti} = primary radical recombination rate constant, k_p = propagation rate constant, k_{td} = termination by disproportionation rate constant, k_{tc} = termination by combination rate constant, k_f = chain transfer to monomer rate constant, and k_s = chain transfer to solvent rate constant.

where λ_k and μ_k are the kth moments of the live and dead polymer chains, respectively.

Applying these simplifications to a set of species mass balances yields the set of working equations shown in Table II. Molar quantities are preferred over concentrations, because significant amounts of solvents or more reactants may be added during a run.

The live and dead moments can also be used to determine the fractional monomer conversion during the batch. Since $(\mu_1 V) + (\lambda_1 V)$ is the total number of moles of monomer in the live and dead chains, the fractional conversion is then

$$x = \frac{(\mu_1 V) + (\lambda_1 V)}{(\mu_1 V) + (\lambda_1 V) + (MV)} \tag{6}$$

Equation (6) is also valid for solution polymerization and when additional monomer is added to the reactor since the extra monomer is accounted for by the differential monomer balance equation.

The cumulative number ($\overline{M}_n$) and weight ($\overline{M}_w$) average molecular weight can then be found by

$$\overline{M}_n = (\lambda_1 + \mu_1)/(\lambda_0 + \mu_0) \tag{7}$$

TABLE II
Mass and Energy Balances for a Semibatch Reactor with Solvent and Monomer Addition

Total mass	$\frac{d(\rho V)}{dt}$	$= \rho_s q_s + \rho_m q_m$ (1)
Monomer	$\frac{d(MV)}{dt}$	$= q_m M_f - \frac{1}{V}(k_p + k_f)(MV)(\lambda_0 V)$ (2)
Initiator	$\frac{d(IV)}{dt}$	$= -k_d(IV)$ (3)
Solvent	$\frac{d(SV)}{dt}$	$= q_s S_f$ (4)
Zeroeth live radical moment	$\frac{d(\lambda_0 V)}{dt}$	$= 2fk_d(IV) - \frac{1}{V}k_t(\lambda_0 V)^2$ (5)
First live radical moment	$\frac{d(\lambda_1 V)}{dt}$	$= 2fk_d(IV) + \frac{1}{V}k_s(SV)[(\lambda_0 V) - (\lambda_1 V)] - \frac{1}{V}k_t(\lambda_0 V)(\lambda_1 V) + \frac{1}{V}(k_p + k_f)(MV)(\lambda_0 V) - \frac{1}{V}k_f(MV)(\lambda_1 V)$ (6)
Second live radical moment	$\frac{d(\lambda_2 V)}{dt}$	$= 2fk_d(IV) + \frac{1}{V}k_s(SV)[(\lambda_0 V) - (\lambda_2 V)] + \frac{2}{V}k_p(MV)(\lambda_1 V) - \frac{1}{V}k_t(\lambda_0 V)(\lambda_2 V) + \frac{1}{V}(k_p + k_f)(MV)(\lambda_0 V) - \frac{1}{V}k_f(MV)(\lambda_2 V)$ (7)
Zeroeth dead polymer moment	$\frac{d(\mu_0 V)}{dt}$	$= \frac{1}{V}k_s(SV)(\lambda_0 V) + \frac{1}{V}k_f(MV)(\lambda_0 V) + \frac{1}{V}(k_{td} + \frac{1}{2}k_{tc})(\lambda_0 V)^2$ (8)
First dead polymer moment	$\frac{d(\mu_1 V)}{dt}$	$= \frac{1}{V}k_s(SV)(\lambda_1 V) + \frac{1}{V}k_f(MV)(\lambda_1 V) + \frac{1}{V}k_t(\lambda_0 V)(\lambda_1 V)$ (9)
Second dead polymer moment	$\frac{d(\mu_2 V)}{dt}$	$= \frac{1}{V}k_s(SV)(\lambda_2 V) + \frac{1}{V}k_f(MV)(\lambda_2 V) + \frac{1}{V}k_t(\lambda_0 V)(\lambda_2 V) + \frac{1}{V}k_{tc}(\lambda_1 V)^2$ (10)
Temperature	$\rho C_p V\frac{dT}{dt}$	$= (-\Delta H_p)\frac{1}{V}(k_p + k_f)(MV)(\lambda_0 V) - UA(T - T_s) + \rho_s C_{ps} q_s(T_f - T) + \rho_m C_{pm} q_m(T_f - T)$ (11)

[a] M = monomer concentration, I = initiator concentration, R· = primary radical concentration, S = solvent conventration, T = temperature, λ_n = nth live radical moment, μ_n = nth dead polymer moment, k_f, k_s = chain transfer rate constants, k_{tc}, k_{td} = termination rate constants, V = reactor volume, q_f = inlet flow rate, f_s = solvent feed fraction, f = initiator efficiency, k_p = propagation rate constant, and k_d = initiation rate constant. T_s = Temperature of the surroundings; T_f = Solvent feed temperature; T_c = Deg °C, T_k = Deg °K.

$$\overline{M}_w = (\lambda_2 + \mu_2)/(\lambda_1 + \mu_1) \tag{8}$$

and the cumulative polymer polydispersity (PD) or heterogeneity index (HI) is given by

$$\mathrm{HI} = \frac{(\lambda_2 + \mu_2)(\lambda_0 + \mu_0)}{(\lambda_1 + \mu_1)^2} \tag{9}$$

Assuming a unimodal distribution, the variance δ of the MWD can be found from the polydispersity and the number average MW by

$$\mathrm{HI} = 1 + (\delta/\overline{M}_n)^2 \tag{10}$$

Hence most of the information about the evolution of the MWD can be obtained without having to generate the entire distribution itself.

Finally, the gel and glass effects are accommodated in the same manner as derived originally in the CCS model and later extended by Louie and Soong.[22,23] The constitutive equations are summarized in Table III. Note that the free volume term for the diffusion-limited termination and propagation rates requires knowledge of the volume fraction of the polymer. This is related to the species concentration in the following way.

By additivity of volumes, the density of the reacting mixture is related to the pure component density by

$$\rho = \Phi_m\rho_m + \Phi_p\rho_p + \Phi_s\rho_s \tag{11}$$

where ρ_m, ρ_p, and ρ_s are the densities of monomer, polymer, and solvent, respectively. The volume fraction of monomer (Φ_m), polymer (Φ_p), and solvent (Φ_s) are computed from the molar quantities by

$$\Phi_m = \frac{(\mathrm{M}V)}{(\mathrm{M}V) + \{(\mu_1 V) + (\lambda_1 V)\}(\rho_m/\rho_p) + (\mathrm{S}V)(\rho_m/\rho_s)(\mathrm{mw}_s/\mathrm{mw}_m)} \tag{12}$$

TABLE III
Constitutive Equations for the Gel and Glass Effects

$$\frac{k_t}{k_t^0} = \frac{C}{C + \Theta_t k_t[\lambda_0]}$$

$$\frac{k_p}{k_p^0} = \frac{C}{C + \Theta_p k_p[\lambda_0]}$$

where

$$C = \exp\left[\frac{(1 - \Phi_p)}{A + B(1 - \Phi_p)}\right]$$

$$A = 0.168 - 8.21E - 6\,(T_c - 114)^2$$

$$B = 0.03$$

$$\Theta_p = 5.4814E - 16 \exp\left(\frac{13982}{T_k}\right)$$

$$\Theta_t = \frac{1.1353E - 22}{[\mathrm{I}_0]} \exp\left(\frac{17420}{T_k}\right)$$

$$\Phi_p = \frac{\{(\mu_1 V) + (\lambda_1 V)\}(\rho_m/\rho_p)}{(MV) + \{(\mu_1 V) + (\lambda_1 V)\}(\rho_m/\rho_p) + (SV)(\rho_m/\rho_s)(mw_s/mw_m)} \quad (13)$$

$$\Phi_s = 1 - \Phi_m - \Phi_p \quad (14)$$

where mw_m and mw_s are the molecular weights of the monomer and solvent, respectively. To complete the calculational procedure, physical properties and rate constants listed in Table IV are used.

The isothermal bulk polymerization of MMA at 70°C with an initiator loading of 0.0258M AIBN serves as the reference case in this study. Under these conditions, reasonably high MW PMMA can be produced within a reasonable batch time. Figure 1 shows the predicted conversion, molecular weight, and polydispersity.

Photoinitiation

Traditional optimum initiation processes have usually varied the small quantities of initiator added continuously into the reacting mixture to adjust initiation rates. However, Chen and Huang[20] noted that it may be difficult to disperse added initiator (which must be carefully metered) uniformly into the reacting mixture, because of the high viscosities encountered at moderate and high conversions. They considered solution polymerization as a means to circumvent the mixing problem. Here we explore another practical approach, i.e., the use of photoinitiation.

Photoinitiation is preferred over the more traditional chemical addition techniques because the sensitizer (or initiator) is uniformly dissolved with the monomer prior to the start of the reaction. Photochemical production of primary radicals can be accurately and precisely controlled by varying

TABLE IV
Rate Constants and Physical Properties

f	= 0.58 for AIBN, f = 1.0 for BPO
k_d	= 6.32×10^{16} exp[(−30.66 kcal/mol)/RT_k] (min^{-1}) AIBN
k_d	= 1.014×10^{16} exp[(−30.0 kcal/mol)/RT_k] (min^{-1}) BPO
k_p^0	= 2.95×10^7 exp[(−4.35 kcal/mol)/RT_k] (L/mol min)
$\frac{k_f}{k_p}$	= 9.48×10^3 exp[(−13.88 kcal/mol)/RT_k]
$\frac{k_s}{k_p}$	= 1.01×10^3 exp[(−11.40 kcal/mol)/RT_k]
k_i^0	= 5.88×10^9 exp[(−0.701 kcal/mol)/RT_k] (L/mol min)
$\frac{k_{tc}}{k_{td}}$	= 3.956×10^{-4} exp[(4.09 kcal/mol)/RT_k]
ρ_m	= $0.968 - 1.225 \times 10^{-3} T_c$ (g/cm^3)
ρ_p	= 1.2 (g/cm^3)
ρ_s	= $0.883 - 9 \times 10^{-4} T_c$ (g/cm^3)
Cp_m	= Cp_p = 0.4 (cal/g °C)
Cp_s	= 0.535 (cal/g °C)
mw_m	= 100.13 (g/mol)
mw_s	= 92.14 (g/mol) for Toluene

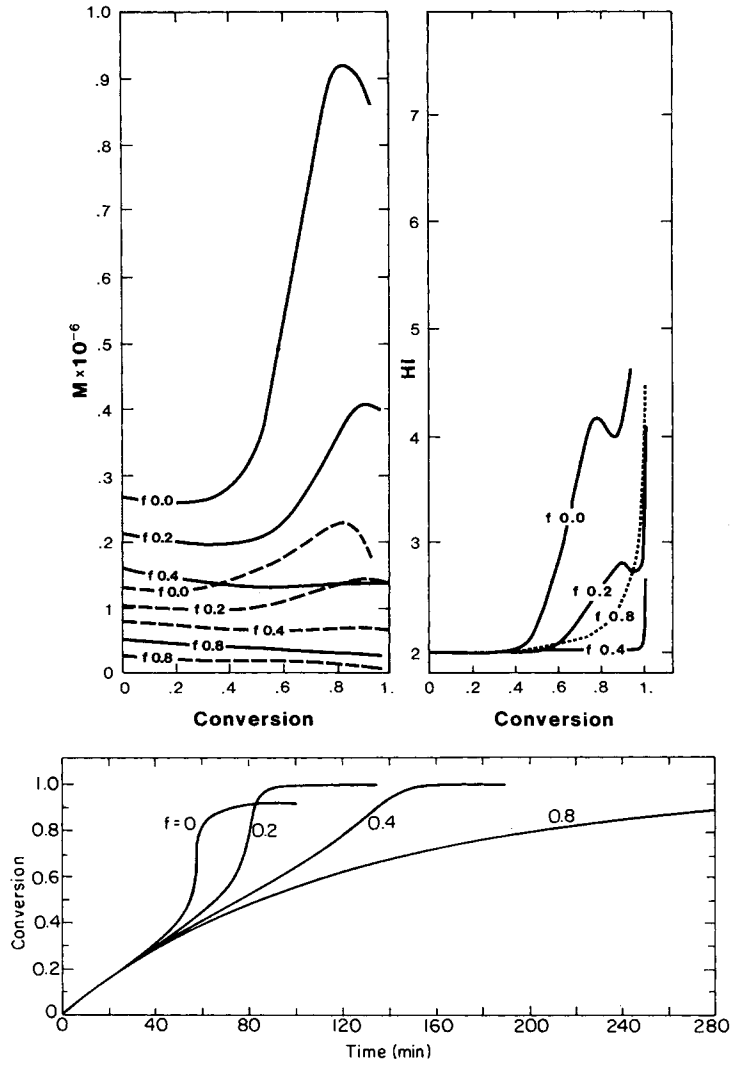

Fig. 1. Predicted conversion, MW, and HI histories for the isothermal batch polymerization of MMA in toluene. $T = 70°C$; $I_0 = 0.0258M$ AIBN. Bottom left: (—) M_w; (- - -) M_n.

the intensity of incident light. Photoinitiation also decouples the initiation process from thermal effects such as dead-ending and thermal runaway. Much lower process temperatures may also be used. Hence, the molecular weight and MWD may be more easily and subtly controlled.

A large number of photoinitiators exist for MMA, among which benzoin is commonly used and will be simulated in this study. High pressure mercury lamps (which radiate in the range around 365 mμ) are usually used as the light source. Uniform initiation throughout the reactor is achieved since PMMA is transparent to UV light, and the initiator loading is low so that radiation absorption is weak over the optical path. Chen et al.[24] successfully used benzoin to initiate MMA in a recent study of the dynamics

of a photo-controlled CSTR. Their kinetic data for benzoin photoinitiation will be used.

To determine the optimum photoinitiation profile for a batch free-radical polymerization, the set of differential species balance equations must be slightly altered to account for photoinitiation. The rate of primary radical formation may be represented by the product of the intensity of light, I_a, and the quantum yield ϕ. After applying the QSSA to primary radicals, the rate of primary radical generation is

$$R_i = k_i[\mathrm{R}][\mathrm{M}] = 2\phi I_a \tag{15}$$

where two primary radicals are formed for each sensitizer molecule. A quantum yield of 1.2×10^{-2} mol of benzoin initiated per Einstein is used.[24] The intensity of light received by the sensitizer is related to the incident light, I_0, by Beer's law:

$$I_a = I_0(1 - \exp(-\xi L\mathrm{s})) \tag{16}$$

where s is the sensitizer concentration, L is the light path of the system, and ξ is the extinction coefficient. Specific geometric factors for a particular reactor can be ignored if the intensity of absorbed light is chosen as the control variable to be optimized. The new mass and energy balance equations to be solved are shown in Table V. Note that chain transfer to the sensitizer is ignored.

Figure 2 shows the conversion, MW, and PD histories for several different objective functions. High conversion is not possible with the minimum PD policy. Conversion sharply increases near the onset of the gel effect and then levels off to a premature limiting conversion. Cause of this sharp increase in reaction rate is due to an increase in the intensity of incident light (see Fig. 3). This surge of primary radical generation counters the decrease in k_t caused by the gel effect with a sudden increase in radical concentration, λ_0. This maintains the kinetic chain length approximately constant. However, k_t drops faster than the rate of initiation in the long run so PD eventually increases. PD can then only be minimized by shutting the reaction down, and this causes the premature limiting conversion.

Turning off the incident light ceases primary radical generation. Macroradicals continue to react, but their lifetimes are extended as the radical concentration declines. This shifts the instantaneous MWD upward and raises PD. To avoid this problem, an inhibitor or a free-radical scavenger such as DPPH should be added as the limiting conversion is reached. Reaction times can be shortened by increasing the temperature. Similar to thermal initiation, MWs increase with decreasing temperature since termination rates fall faster than propagation rates.

Higher conversions can be obtained with a constant propagation-rate initiation policy [eq. (2)]. The constant rate of propagation results in a steady conversion rise with time. The sudden autoacceleration caused by the gel effect is smoothed out by drastically reduced rates of photoinitiation (see Fig. 3). Photoinitiation increases again when the rate of propagation falls

TABLE V
Mass and Energy Balances for a Batch Reactor with Photoinitiation

Total mass	$\frac{d(\rho V)}{dt} = 0$	(1)
Monomer	$\frac{d(MV)}{dt} = -\frac{1}{V}(k_p + k_f)(MV)(\lambda_0 V)$	(2)
Sensitizer	$\frac{d(sV)}{dt} = -\phi I_a$	(3)
Zeroeth live radical moment	$\frac{d(\lambda_0 V)}{dt} = 2f\phi I_a - \frac{1}{V}k_t(\lambda_0 V)^2$	(4)
First live radical moment	$\frac{d(\lambda_1 V)}{dt} = 2f\phi I_a - \frac{1}{V}k_t(\lambda_0 V)(\lambda_1 V) + \frac{1}{V}(k_p + k_f)(MV)(\lambda_0 V) - \frac{1}{V}k_f(MV)(\lambda_1 V)$	(5)
Second live radical moment	$\frac{d(\lambda_2 V)}{dt} = 2f\phi I_a + \frac{1}{V}k_p(MV)[(\lambda_0 V) + 2(\lambda_1 V)] + \frac{1}{V}k_f(MV)[(\lambda_0 V) - (\lambda_2 V)] - \frac{1}{V}k_t(\lambda_0 V)(\lambda_2 V)$	(6)
Zeroeth dead polymer moment	$\frac{d(\mu_0 V)}{dt} = \frac{1}{V}k_f(MV)(\lambda_0 V) + \frac{1}{V}\left(k_{td} + \frac{1}{2}k_{tc}\right)(\lambda_0 V)^2$	(7)
First dead polymer moment	$\frac{d(\mu_1 V)}{dt} = \frac{1}{V}k_f(MV)(\lambda_0 V) + \frac{1}{V}k_t(\lambda_0 V)(\lambda_1 V)$	(8)
Second dead polymer moment	$\frac{d(\mu_2 V)}{dt} = \frac{1}{V}k_f(MV)(\lambda_2 V) + \frac{1}{V}k_t(\lambda_0 V)(\lambda_2 V) + \frac{1}{V}k_{tc}(\lambda_1 V)^2$	(9)
Temperature	$\rho C_p V\frac{dT}{dt} = (-\Delta H_p)\frac{1}{V}(k_p + k_f)(MV)(\lambda_0 V) - UA(T - T_s)$	(10)

due to the glass effect. Reaction stops when a glass is formed. MW and PD of the polymer produced are both much larger than those obtained by conventional thermal initiation techniques. Extremely long chains are produced by the few radicals present during the gel effect. This produces a bimodal distribution and skews the MWD toward higher MWs.

As seen in Figure 3, a constant number or weight average MW policy produces results similar to that of a constant PD policy. All policies fail around the onset of the gel effect when MW begins to drift and PD broadens. The constant rate policy, however, reaches a higher conversion and MW, at the expense of a broad PD (and hence a wide MWD). Conventional thermal initiation also produces a higher PD than the minimum PD policy, but has a higher overall conversion and MW. Of the various objective functions, only the minimum PD policy controls both the MW and narrows the MWD. Since this is the major objective of our optimization, we shall define the minimum PD policy as being the optimal batch history.

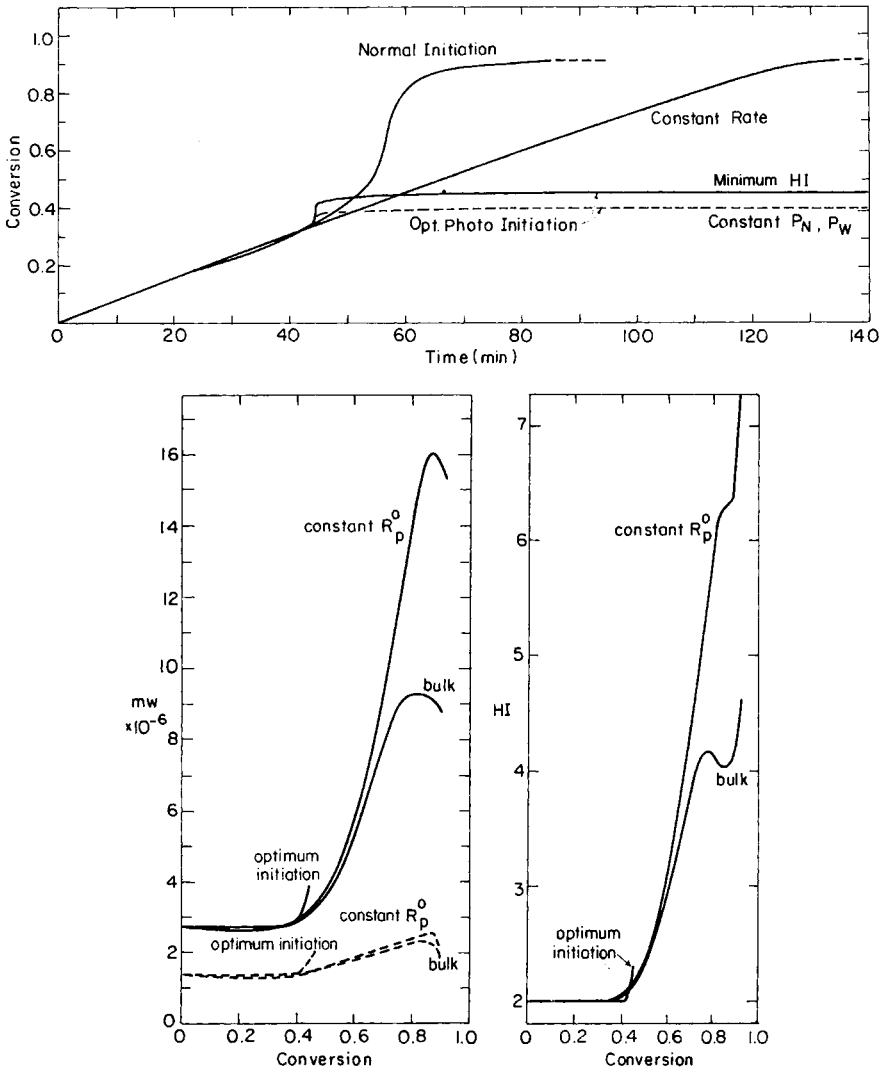

Fig. 2. Comparison of optimum (minimum HI) isothermal photoinitiation with isothermal bulk, constant reaction rate, and constant $\overline{M}_n$ and $\overline{M}_w$ polymerization policies. $T = 70°C$; $s = 0.0258M$ benzoin. A constant rate bulk polymerization policy leads to higher MWs and HI than either an uncontrolled isothermal or minimum HI polymerization. Bottom left: (—) M_w; (- - -) M_n.

Strikingly different behavior occurs when heat transfer is no longer ideal, i.e., when the system becomes nonisothermal. Reactor temperatures will then be determined from an overall energy balance. This influences the optimum operating history through the kinetic rate constants. Different reaction histories are possible depending on the overall heat transfer coefficient used. In our simulations, heat transfer will be to a constant temperature, cooling water jacket set at the initial reactor temperature (70°C).

Complete conversion is now possible (see Fig. 4) using the minimum PD policy. The desired MW is obtained, even at high temperatures. This re-

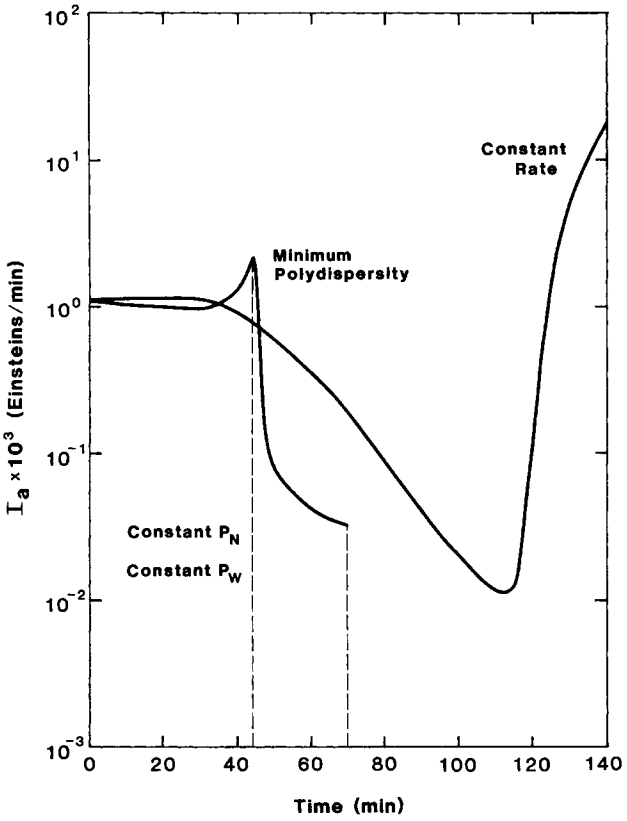

Fig. 3. Variation of the intensity of absorbed light for various photopolymerization policies. Notice that a constant $\overline{M}_n$ and $\overline{M}_w$ policy is identical to a minimum HI policy for most of the polymerization.

quires the intensity of incident light to fall toward extinction (see Fig. 5) in an effort to compensate for the high kinetic rates. A premature limiting conversion occurs under adiabatic conditions because there exists a limiting critical temperature above which the minimum PD policy dictates that the optimum radical concentration should drop to zero (see Fig. 6).

As heat transfer is introduced, the maximum temperature falls below the critical temperature, and complete conversion is possible. The rate of polymerization is quite slow at the low radical concentrations needed to keep MW constant (curve 2 in Fig. 4). The optimal light intensity is relatively high initially, but must drop by an order of magnitude as the critical temperature is approached. A glass is formed upon cooling the reaction mixture below its glass transition temperature.

Faster rates are possible with improved heat removal rate (curves 3–5). Much sharper conversion and temperature profiles are generated. Because the gel effect shifts MW upwards more than high temperature shifts the instantaneous MW downwards, photoinitiation rates must increase with increasing system temperature to hold MW and PD constant. The optimum initiation profiles exhibit a single sharp burst of light just at the onset of

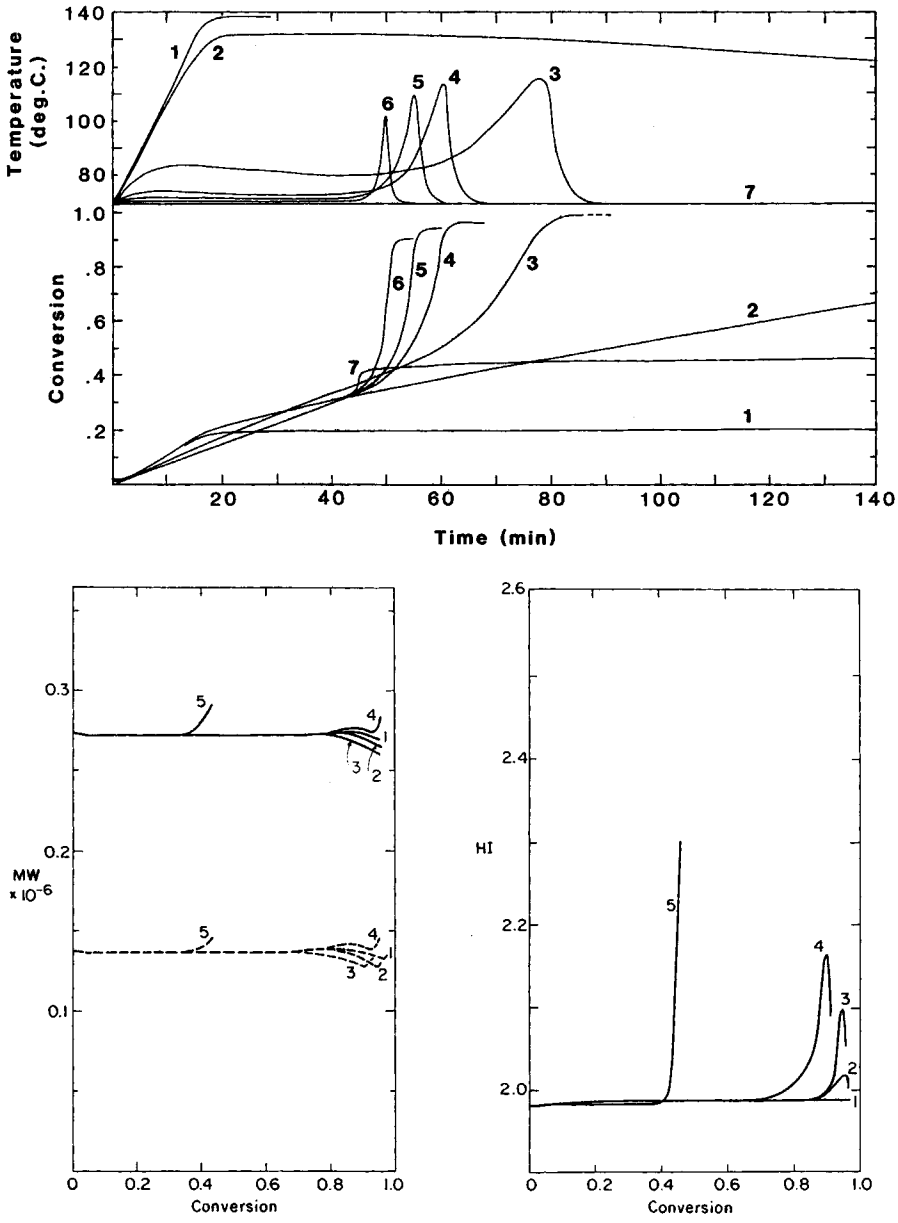

Fig. 4. Influence of heat transfer coefficient on the optimum (minimum HI) nonisothermal photopolymerization of MMA. T = 70°C; s = 0.0258M benzoin; V_0 = 0.5 L; A = 483.6 cm². Multiply U(Btu/h ft² °F) by 4.88 to convert to U(kcal/h m² °C). Notice much higher conversions are possible under nonisothermal conditions than with isothermal ones. U(Btu/h ft² °F): top—(1) 0; (2) 1; (3) 10; (4) 30; (5) 50; (6) 100; (7) ∞; bottom right—(1) 0; (2) 30; (3) 50; (4) 100; (5) ∞. Bottom left: (—) M_w; (- - -) M_n.

the gel effect. A limiting conversion is reached as glass formation occurs before complete conversion.

Under near-isothermal conditions, premature limiting conversions once again reduce polymer yields (curves 6 and 7). The high rates of heat transfer

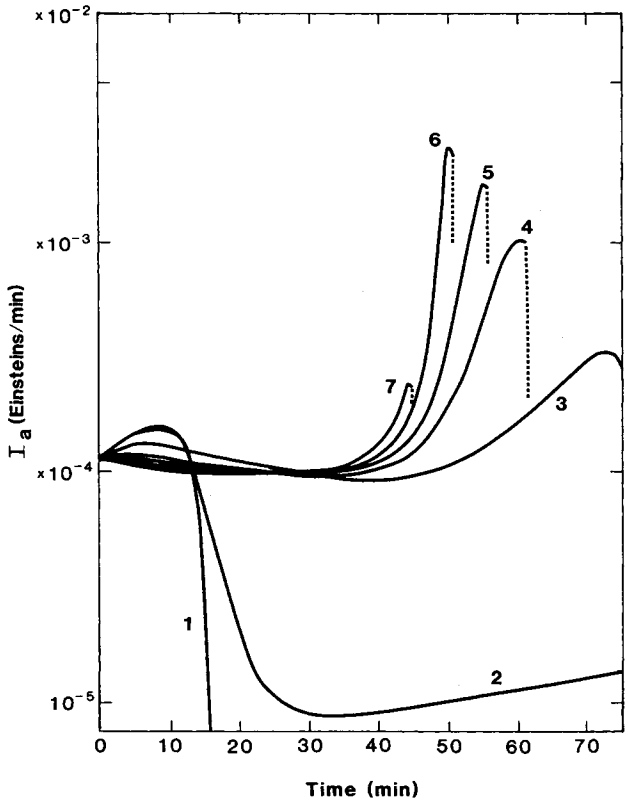

Fig. 5. Effect of heat transfer coefficient on the optimum nonisothermal photoinitiation profile. Conditions are the same as in Figure 4. U (Btu/h ft² °F): (1) 0; (2) 1; (3) 10; (4) 30; (5) 50; (6) 100; (7) ∞.

do not allow MW to remain constant during the gel effect. An increase in the light intensity alone cannot compensate for the decrease in k_t unless the rate of termination can be increased by either raising the temperature or increasing the radical concentration or both. In the limit of isothermal temperatures, radical populations must increase by orders of magnitude almost instantaneously (see Fig. 6). Since this is not possible, initiation is halted, and the run aborted to prevent PD from increasing.

Process Temperature

Temperature can be used to control the instantaneous MW by varying the ratio of the rate of propagation to the rate of thermal initiation. The MWD can thus be narrowed or broadened depending on the reactor temperature history. Species balances equations for a batch reactor with temperature control are the same as the ones for an uncontrolled semi-batch reactor, with the exception of the energy balance (see Table II). AIBN is again used as the thermal initiator in the following simulations.

The optimum temperature and conversion profiles are shown in Figure 7 along with the equivalent isothermal and adiabatic cases for comparison. Conversions comparable to isothermal polymerizations can be achieved in

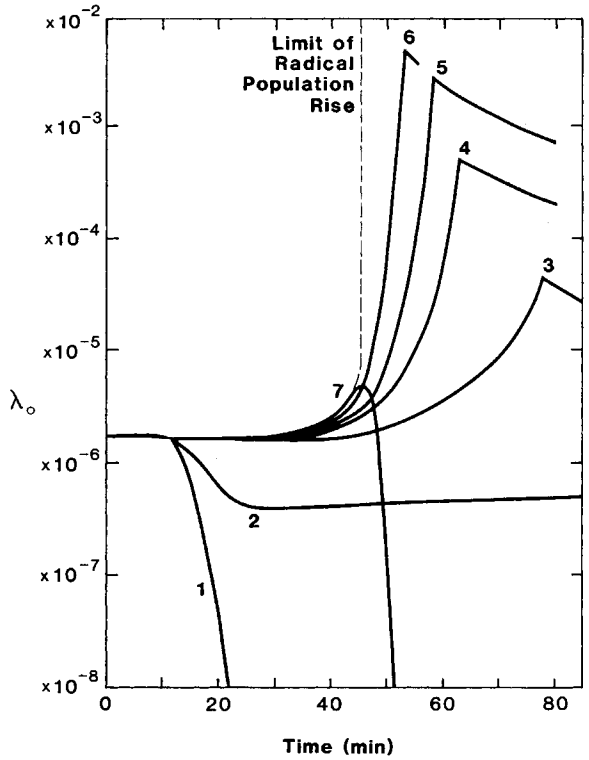

Fig. 6. Variation of the total radical population with time at different heat transfer rates for the nonisothermal photopolymerization of MMA. High conversions are not possible under isothermal conditions because the radical population cannot increase fast enough. U (Btu/h ft² °F): (1) 0; (2) 1; (3) 10; (4) 30; (5) 50; (6) 100; (7) ∞.

a shorter time with the minimum PD policy. The optimum temperature must decrease slightly at low conversions due to volume contraction, causing a rise in all reactant concentrations. Otherwise, thermal drift caused by the increase in initiator concentration would broaden the MWD. As the gel effect becomes significant, the temperature gradually rises to promote termination. This maintains the instantaneous MW constant in the early part of the gel effect. However, as the glass effect begins, reactor temperature must drop sharply to freeze the reaction mixture into a glass. With both k_p and k_t falling during the latter part of the gel effect, shorter chains will always be produced, and this broadens the MWD. Increasing the temperature to eliminate the glass effect fails, in this case, since the rate of termination rises faster than the rate of propagation. This broadens the MWD by producing smaller chains. The glass effect may be eliminated by the optimum policy at lower desired MWs.

From Figure 7, the minimum PD policy essentially holds MW constant until around 60% conversion. Then, $\overline{M}_w$ begins to rise, and PD increases due to the glass effect. The amount of high MW material produced is minimized by the sudden drop in reaction temperature. The final PD is much lower than that of the isothermal PD. The adiabatic PD is greater than both cases because $\overline{M}_n$ drops faster than $\overline{M}_w$ throughout the polymerization.

The temperature rise for the optimal policy does not lead to dead-ending of the polymerization. Dead-ending to minimize the batch time as proposed by Sachs et al.[18] and Chen et al.[19,20] is not recommended for PMMA. As shown by the adiabatic simulation, high conversions are usually not reached; MW is low; and fairly high PDs are obtained with dead-ending. Part of the problem lies in the selection of a proper objective function. Control of the MWD is usually overlooked in formulating minimum end-time policies. Chen et al.[19,20] experimentally found that the MWD was not significantly broadened by the use of the optimum minimum end-time policy, as measured by the viscosity average MW. No comparison with the minimum polydispersity was made. Wu et al.[17] experimentally determined the MWD by GPC in their study and found PD to increase with conversion when the minimum end-time policy was imposed.

These observations indicate that the optimum batch time for PMMA may be drastically different from previously proposed minimum end-time policies. Since producing the narrowest MWD is of prime importance, we recommend that batch times can only be reduced by minimizing the endtimes of the minimum PD policies. This motivated us to study the effects of

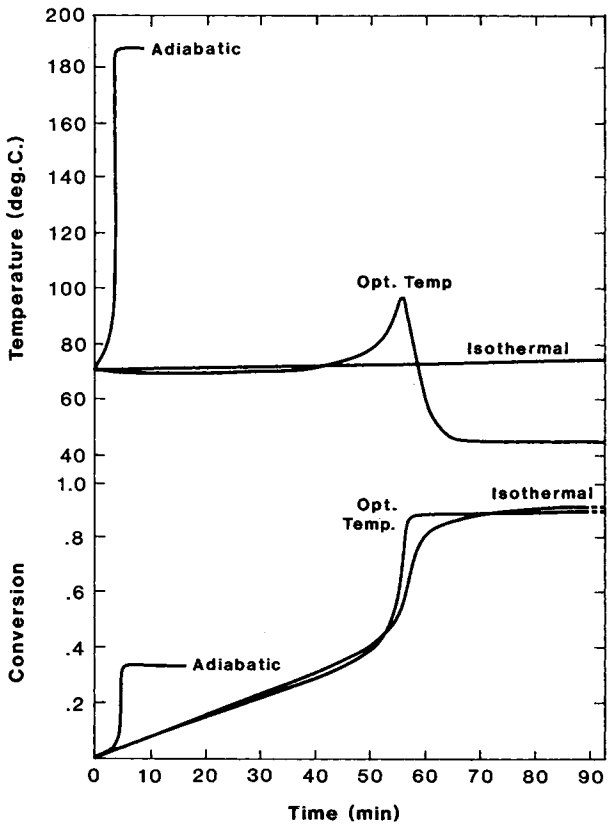

Fig. 7. Comparison of the optimum (minimum HI) temperature policy with adiabatic and isothermal bulk polymerization. T_0 = 70°C, I_0 = 0.0258M AIBN, V_0 = 0.5 L, A = 483.6 cm^2. Notice that the glass effect increases HI at high conversions. Middle: (—) M_w; (- - -) M_n.

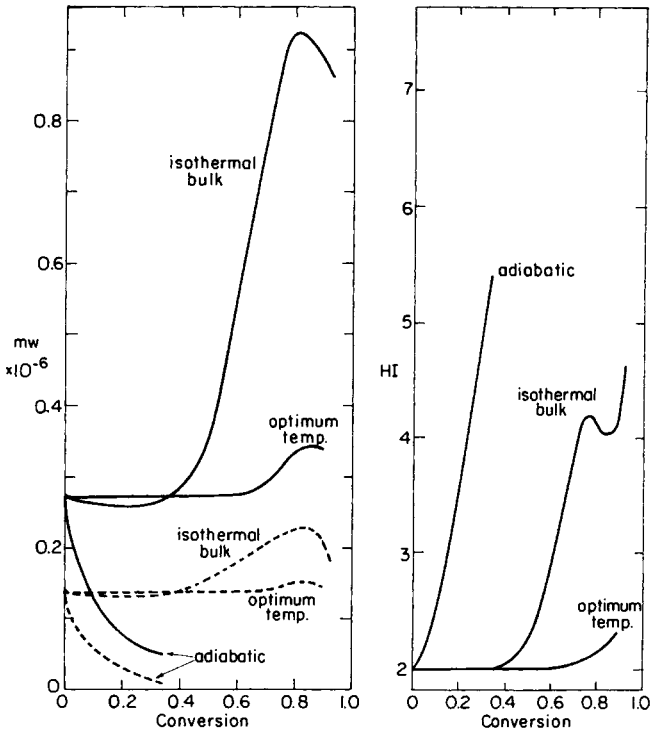

Fig. 7. *(continued from previous page)*

initiator loading and process temperature on the optimum temperature, initiation, and monomer and solvent addition profiles.

Different desired MWs can be obtained by varying either the starting AIBN loading, or the initial reactor temperature T_0 (for a given loading), while following the respective optimum temperature policy. Only one initiator loading exists for a given MW and T_0. This is in agreement with the minimum end-time study of Chen and Jeng.[19] Faster batch times can be obtained at higher initial temperatures, but only at the expense of lower final MWs. At sufficiently high initial temperatures ($T_0 > 114$°C), the glass effect is eliminated altogether and the optimum temperature profile will then resemble a monotonically increasing function.

The effect of initiator loading on the optimum profile is shown in Figure 8. Slightly lower maximum reactor temperatures and sharper excursions are required at higher initiator loadings. Lower temperatures can be used since more initiation occurs. This offsets rises in both $\overline{M}_n$ and $\overline{M}_w$ and controls PD. At lower initiator loadings, slightly higher conversions are obtained, but higher temperatures and broader rises are needed. This leads to larger final PD.

Monomer Addition

Monomer may be added during the polymerization to maintain a constant monomer to initiator concentration ratio. Drift of the instantaneous MWD is minimized, as the kinetic chain length is held constant. This narrows

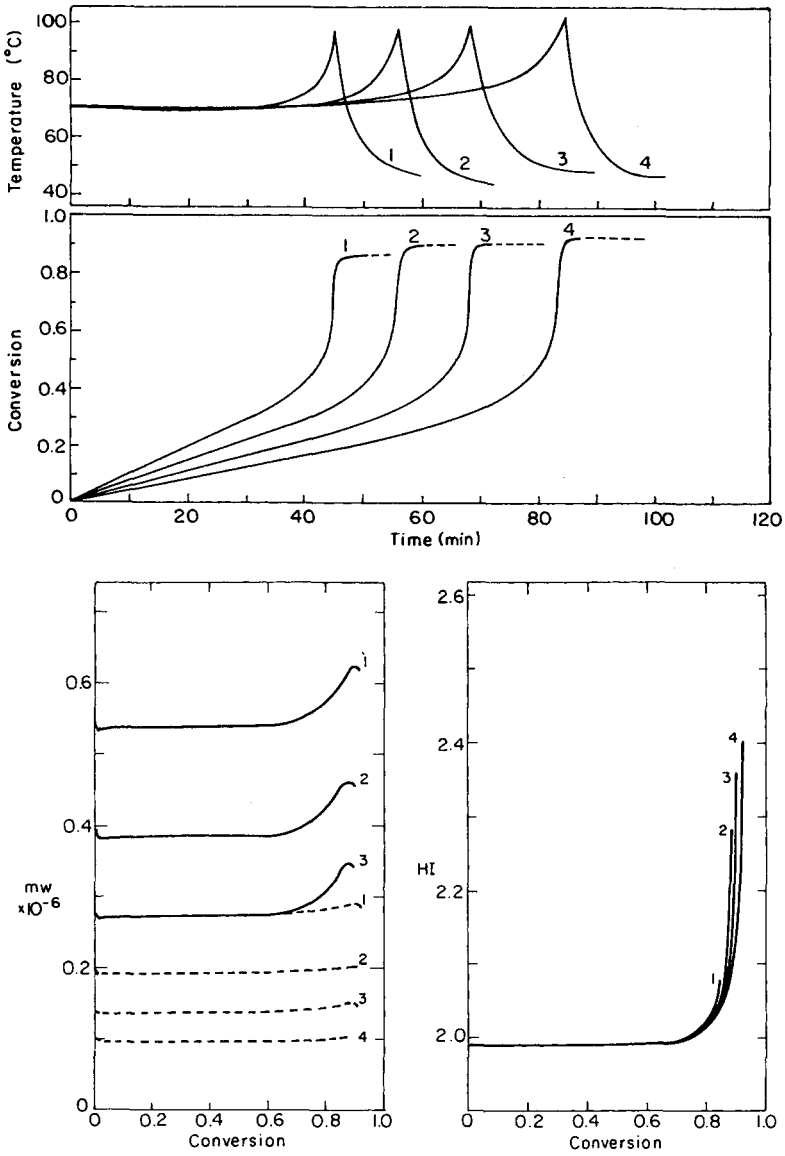

Fig. 8. Influence of initiator loading on the optimum temperature policy and conversion history. Same conditions prevail as in Figure 7. Note that MW can be adjusted independent of HI by changing I_0. I_0 M AIBN: Top—(1) 0.05160; (2) 0.02580; (3) 0.01290; (4) 0.00645; bottom right: (1) 0.00645; (2) 0.01290; (3) 0.02580; (4) 0.05160. Bottom left: (—) M_w; (- - -) M_n.

the cumulative MWD. In addition, since MMA is a solvent for PMMA, it was hoped that monomer addition would exploit some of the advantages of solvent addition while eliminating the need for solvent recovery. Model equations for a semibatch, monomer addition reactor are shown in Table II. Monomer conversion, as we have defined it, will include all the monomer added to the reactor since the start, plus the amount initially present [see eq. (6)].

A comparison of ordinary bulk polymerization with the optimum monomer addition profile with and without the gel and glass effects is shown in Figure 9. As proposed by Hoffman et al.,[7] the MWD can be controlled by monomer addition to high conversions when the gel effect is absent. Monomer flow begins almost from the start, but tapers off throughout the rest of the batch. Reaction rates are slowed by dilution of the initiator. Both number and weight average MWs are held constant by maintaining a steady monomer to initiator ratio in the absence of the gel and glass effects. A second large monomer addition occurs at high conversions when concentration drift due to monomer depletion must be avoided. In practice, this second addition peak would not be added and the reaction stopped by the use of a free-radical scavenger. For clarity, this peak has been omitted from Figure 9.

However, inclusion of the gel and glass effects drastically changes such optimistic results. Figure 9 illustrates the importance of the two effects. Low limiting conversions now characterize the polymerization. Small amounts of monomer are added initially to compensate for the volume contraction. Monomer conversion increases linearly until the onset of the gel effect. The final conversion is limited since a sudden drop in k_t can only be prevented by increasing the free volume of the reacting mixture. Addition of monomer maintains the apparent conversion and avoids the gel effect. Monomer flow dilutes the initiator and stops the polymerization. As the AIBN concentration drops, the instantaneous polymer molecular weights increase and the MWD broadens. PD can be minimized by adding more AIBN with the MMA to hold the initiator concentration constant or by

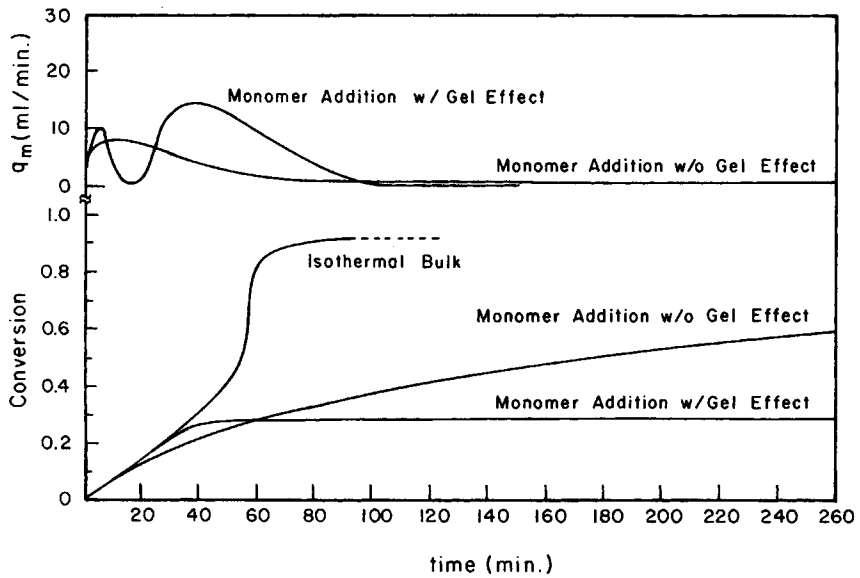

Fig. 9. Comparison of optimum (minimum HI) monomer addition with and without gel effect with uncontrolled isothermal bulk polymerization. $T = 70°C$; $I_0 = 0.258M$ AIBN. The minimum HI policy fails when k_p begins to drop due to the glass effect. Bottom left: (—) M_w; (- - -) M_n.

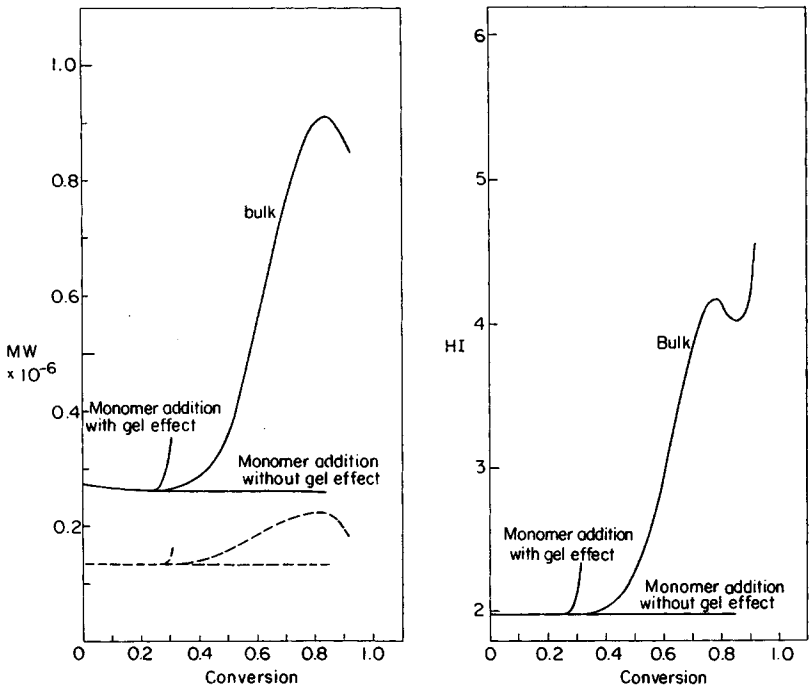

Fig. 9. *(continued from previous page)*

adding a radical scavenger to stop the polymerization. Little advantage is accrued by using monomer addition over ordinary bulk polymerization, if the potential threat of the gel effect is not neglected.

Solvent Addition

Addition of a solvent to control the polymerization has traditionally been shunned because it introduces a new component which often must be removed to obtain the pure polymer. Small traces of solvent usually remain as impurities since no separation is perfect. However, work done by Gutowski et al.[25] has shown that the solvent may be efficiently separated with an energy-conserving liquid–liquid phase separation. Carra et al.[26] have demonstrated that other volatile residues can also be removed during solvent separation to enhance polymer purity. A better separation can be obtained with an appropriate choice of solvent and subsequent operating conditions. Hence, solvent addition may still be a candidate control strategy for optimizing MWD.

Solvent affects the reaction in several ways. Addition of a solvent limits the instantaneous MW via chain transfer. This controls the upward drift of the instantaneous MW during the gel effect. More importantly, the gel effect itself can be reduced or eliminated by using solvent to increase the available free volume.[27] Hence, higher conversions without increases in PD are possible. Solvent also improves mixing of the various reactants by lowering the bulk viscosity of the reacting mixture. In addition, it eliminates the glass effect, so the product is easier to handle.

Model equations for a semibatch reactor with solvent addition are shown in Table II. These are solved along with the polydispersity constraint as the objective function to yield the optimum solvent addition profiles. Specific solvent characteristics are incorporated in the constitutive equation for heat capacity and density. Toluene is chosen as the solvent for our study, since it is a good solvent for PMMA.

Isothermal Solvent Addition

The polymerization begins in the bulk mode. No solvent is needed until the onset of the gel effect. Conversion increases linearly with time suggesting that the optimum policy maintains a constant rate of polymerization for most of the reaction. Near complete conversion with almost constant MW can be obtained using the optimum solvent addition profile (see Figs. 10 and 11).

The advantages of selective solvent addition are quite apparent when compared with the equivalent straight solution polymerization. Both cases end up with the same total solvent content in the final product. In the programmed addition reaction, polymer MWs are kept high, and the amount of solvent needed to control the gel effect is minimized by delaying the addition of solvent for as long as possible. MW and PD remain fairly constant until very high conversions are reached when concentration drift due to monomer depletion begins to drop $\overline{M}_n$. Such optima cannot be achieved with the equivalent solution case, where the solvent is present initially. MWs are low from the start of the reaction due to chain transfer. In addition, the gel effect is still present to raise MWs (and broaden the MWD) and to negate part of the strong concentration drift encountered at high conversion.

Both straight solution polymerization and solvent addition cases require much longer batch times than a similar uncontrolled bulk reaction, since the addition of a solvent dilutes both monomer and initiator concentrations and lowers the rate of propagation. Reaction rates are initially faster in the optimum case than with straight solution. However, autoacceleration of the rate by the gel effect allows the solution polymerization to be completed at just about the same time as the programmed solvent addition case.

The optimum solvent addition profile resembles an inverted parabola. Solvent flow begins at the onset of the gel effect and increases sharply until the gel effect is sufficiently suppressed. Flow drops off as the reaction nears completion. As monomer depletion begins to affect the number average MW, tremendous amounts of solvent are needed to dilute the remaining initiator to maintain high MWs and minimize PD. This results in a huge secondary solvent peak. In actual experimental practice, this peak may be discarded without changing the overall outcome (see Fig. 10). For clarity, this peak has been omitted from all optimum flow profiles. A radical scavenger (like DPPH) could alternatively be used to terminate the batch.

Increasing reaction temperatures leads to shorter batch times for isothermal programmed solvent injection runs (see Figs. 12 and 13). Product MWs again fall due to higher initiator decomposition rates. Average MWs

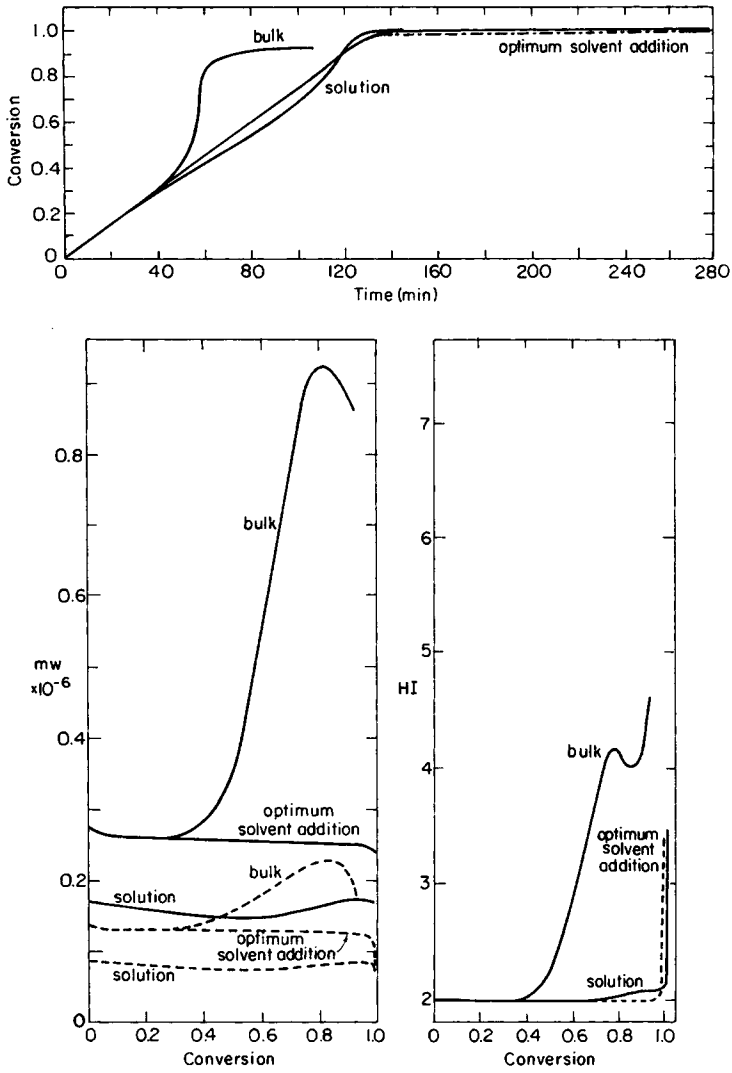

Fig. 10. Comparison of the optimum (minimum HI) isothermal solvent addition policy with bulk and equivalent solution ($f_s = 0.36$) polymerization cases. $T = 70°C$; $I_0 = 0.0258M$ AIBN; $V_0 = 0.5$ L.) Notice that the gel effect is still present in the equivalent solution case. Bottom left: (—) M_w; (- - -) M_n.

remain constant, but the minimum PD increases slightly with increasing temperature as a result of the temperature dependence of k_{td}/k_{tc}.

Solvent addition profiles narrow with increasing temperature. Faster addition rates are needed to keep pace with the faster reaction. Surprisingly, less total solvent is needed at higher temperatures for the same amount of monomer reacted (see Fig. 12). This is in fact reasonable as solvent and radical mobility both increase with temperature. Less solvent is thus needed to improve chain mobility further. Hence, a tradeoff exists between using more solvent or decreasing initiator loading and employing higher temperatures to obtain the desired MW. If energy costs are low, higher tem-

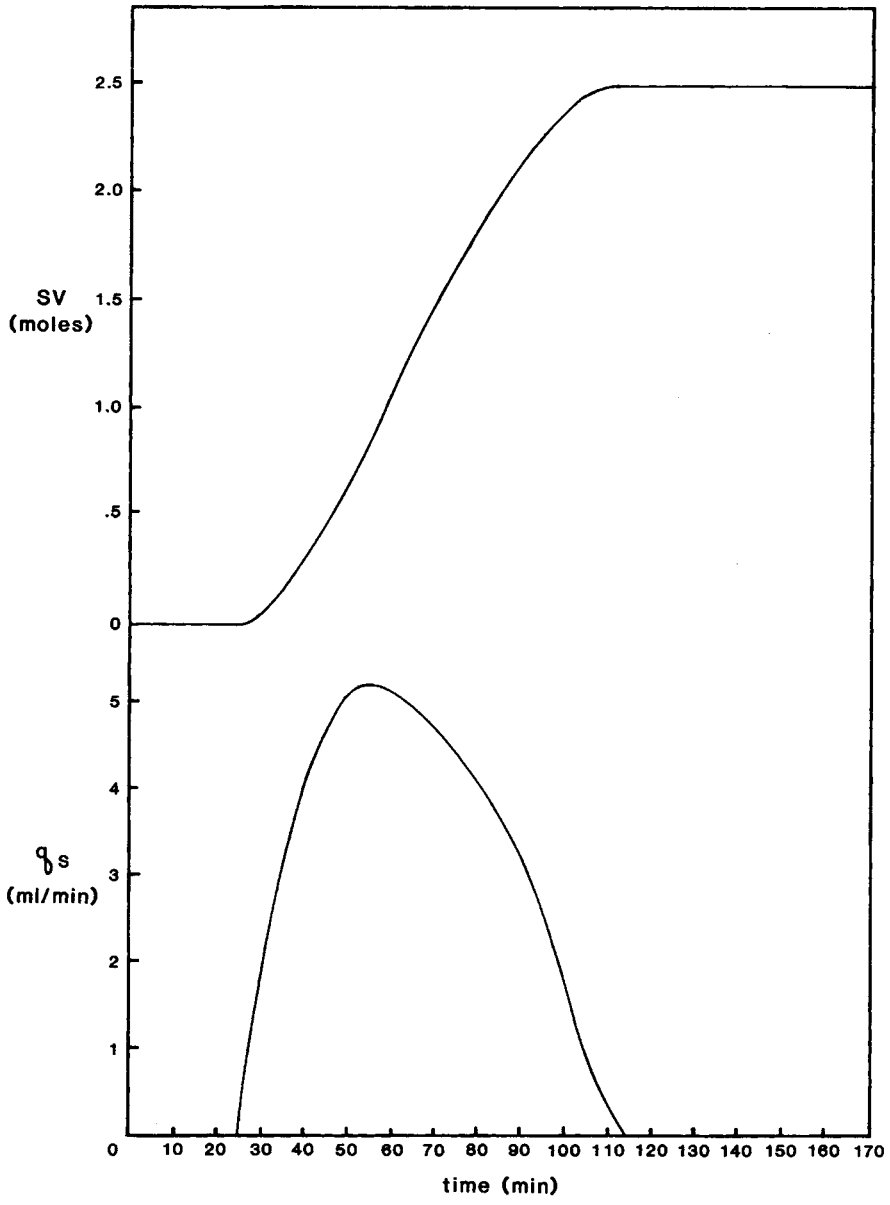

Fig. 11. The optimum isothermal solvent addition flow profile. The large secondary solvent peak needed to avoid the glass effect (which is unrealistic in actual practice) has been ignored. Toluene is the simulated solvent. $I_0 = 0.0258M$ AIBN; $T = 70°C$; $V_0 = 500$ mL MMA.

peratures are favored. Otherwise, the use of more solvent depends upon the amount of subsequent solvent separation required (as this step is also energy-intensive). The optimum temperature must be determined from an overall economic optimization of the whole process.

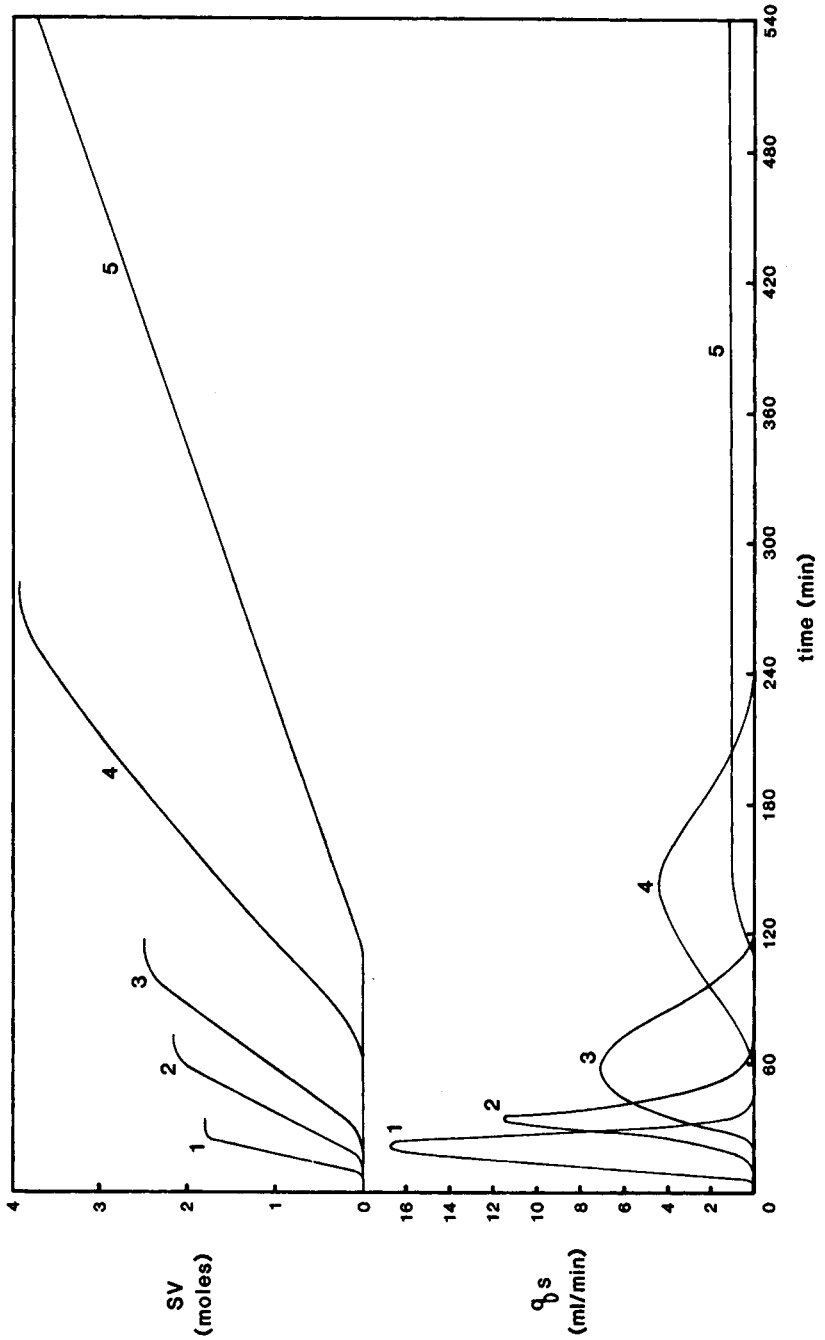

Fig. 12. Influence of reaction temperature on the optimum isothermal solvent addition policy and conversion history. $I_0 = 0.0258M$ AIBN; $V_0 = 500$ ml MMA. Note less solvent is needed at higher temperatures (°C): (1) 90; (2) 80; (3) 70; (4) 60; (5) 50.

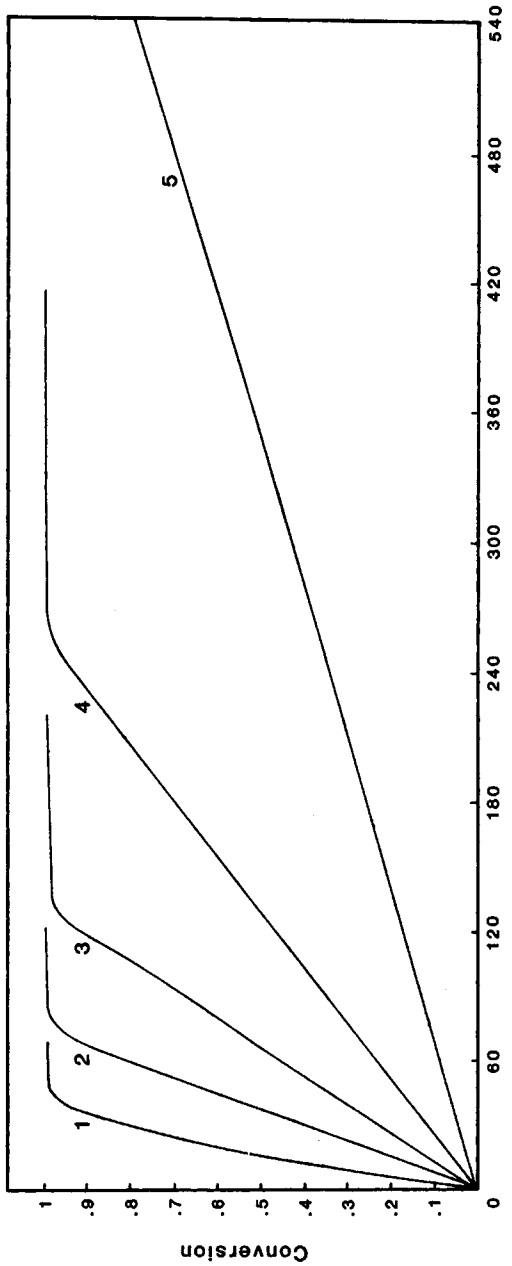

Fig. 12. *(continued from previous page)*

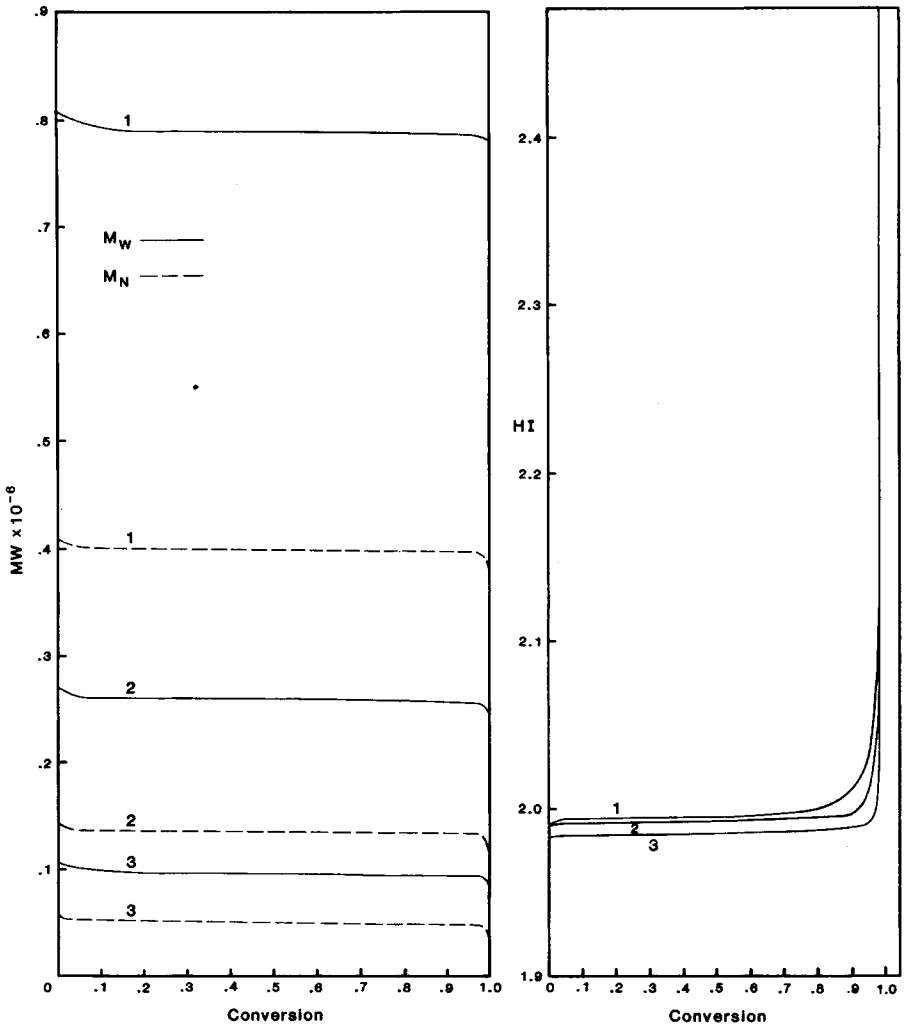

Fig. 13. The effect of reaction temperature on the molecular weight and polymer polydispersity produced by optimum isothermal solvent addition. Left: (—) M_w; (- - -) M_n. Right: I_0 = 0.0258M AIBN; V_0 = 500 ml MMA T (°C): (1) 50; (2) 70; (3) 90.

Ito[28] noted that onset of the gel effect varies slightly with the initiator loading. This could have some effect on the optimum solvent addition profile. With low loadings, solvent profiles tend to be broad since the polymerization proceeds slowly. Addition peaks narrow rapidly with increasing loading and reaction rate (see Figs. 14 and 15). The optimum solvent peak shifts to shorter times with increasing initiator concentration. Faster batch times are again realized at the expense of lower product molecular weights, when the initiator loading is increased.

Contrary to our intuition, the amount of solvent needed to control the gel effect decreases at higher initiator concentrations. This suggests that solvent may be conserved by using more initiator. The only compromise is the lowering of product MW. However, the simulation indicates that the

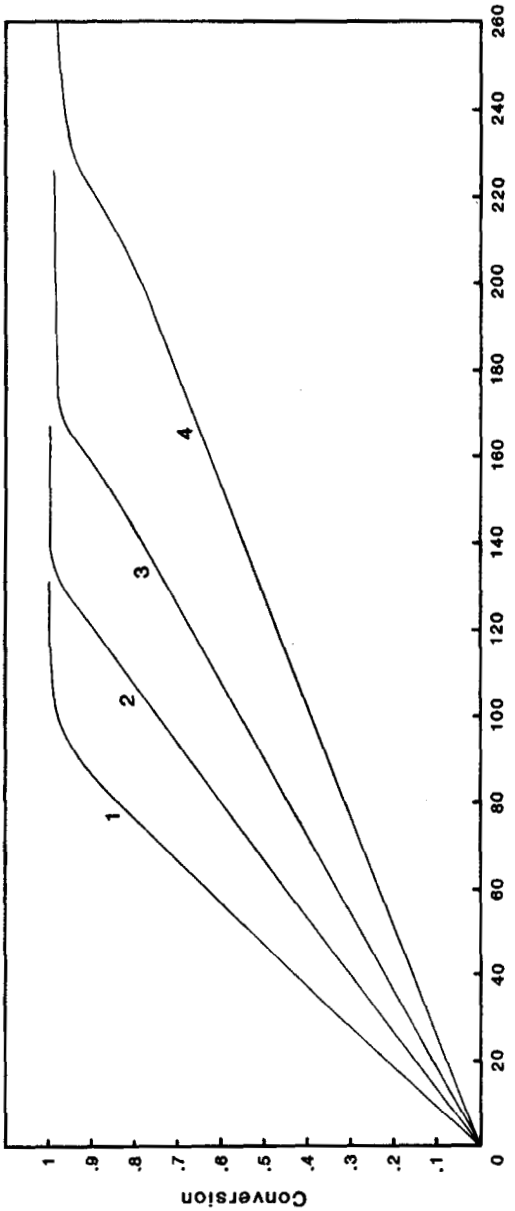

Fig. 14. Influence of initiator loading on the optimum isothermal solvent addition policy. $T = 70°C$; $V_0 = 0.5$ L. Note that MW can be adjusted independent of HI by changing I_0 (M AIBN): top—(1) 0.0516; (2) 0.0258; (3) 0.0129; (4) 0.00645; bottom: (1) 0.0516; (2) 0.0258; (3) 0.0129; (4) 0.00645.

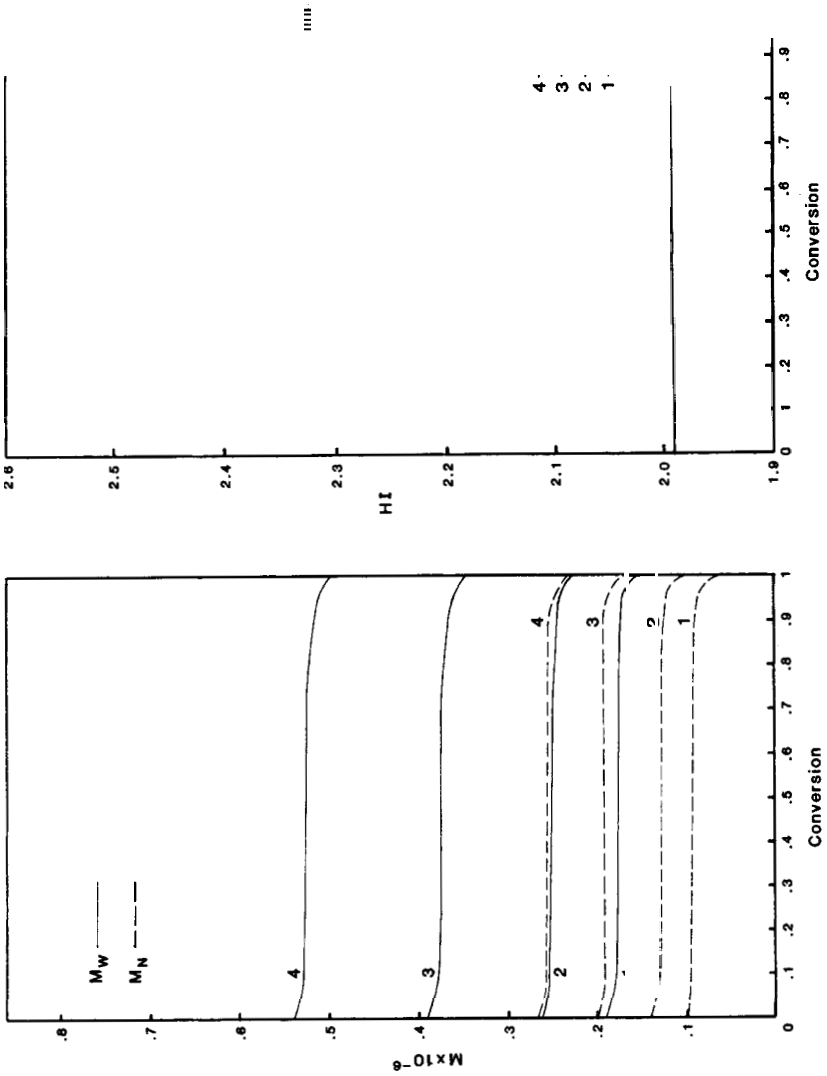

Fig. 14. *(continued from previous page)*

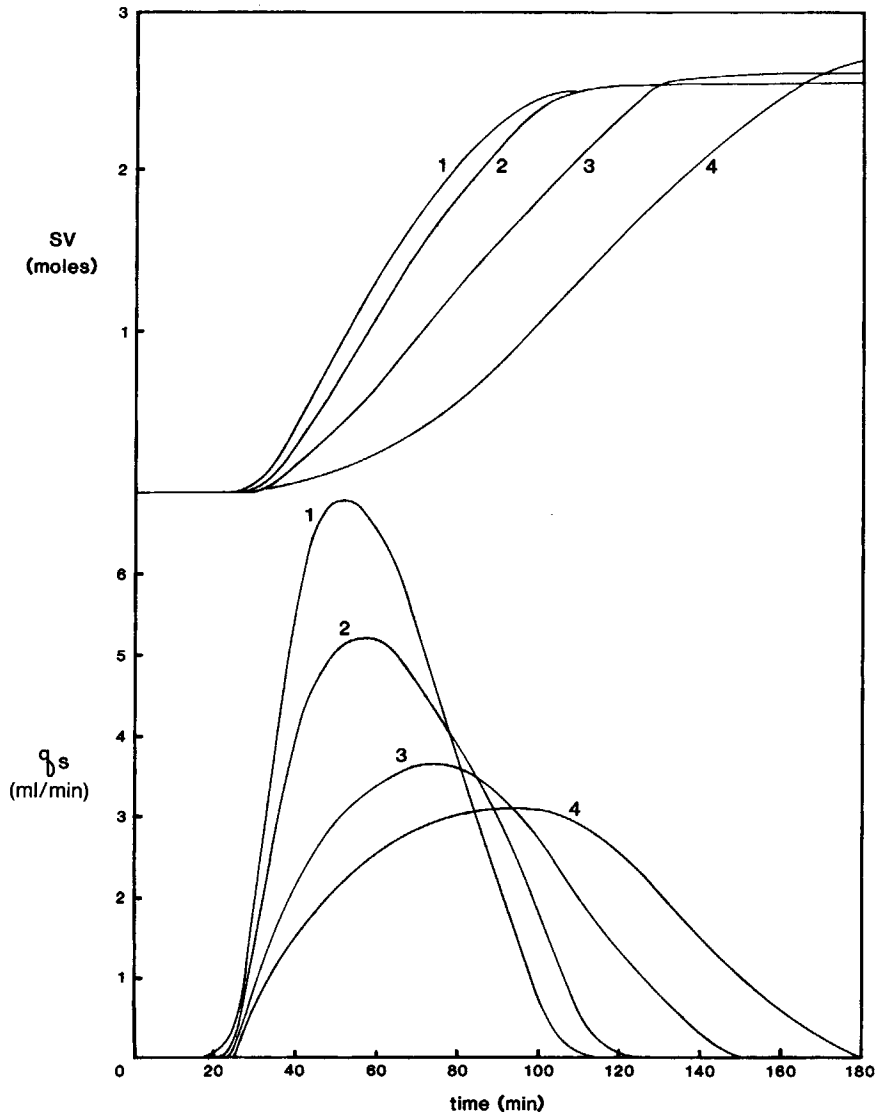

Fig. 15. Variation of the optimum solvent addition profile with initiator loading. Only a mild dependence on I_0 (M AIBN) exists for the optimum flow profile: (1) 0.0516; (2) 0.0258; (3) 0.0129; (4) 0.00645.

MW decreases substantially for each incremental solvent saved. Thus, it is necessary to specify the minimum product MW (with the narrowest MWD).

A wide variety of new optimum profiles emerges when the polymerization procedes under nonisothermal conditions (see Figs. 16–20). Reaction temperatures are again determined from an overall energy balance, with solvent added at the surrounding temperature (unless otherwise specified). Conversion tends to increase linearly with time when the heat transfer rate

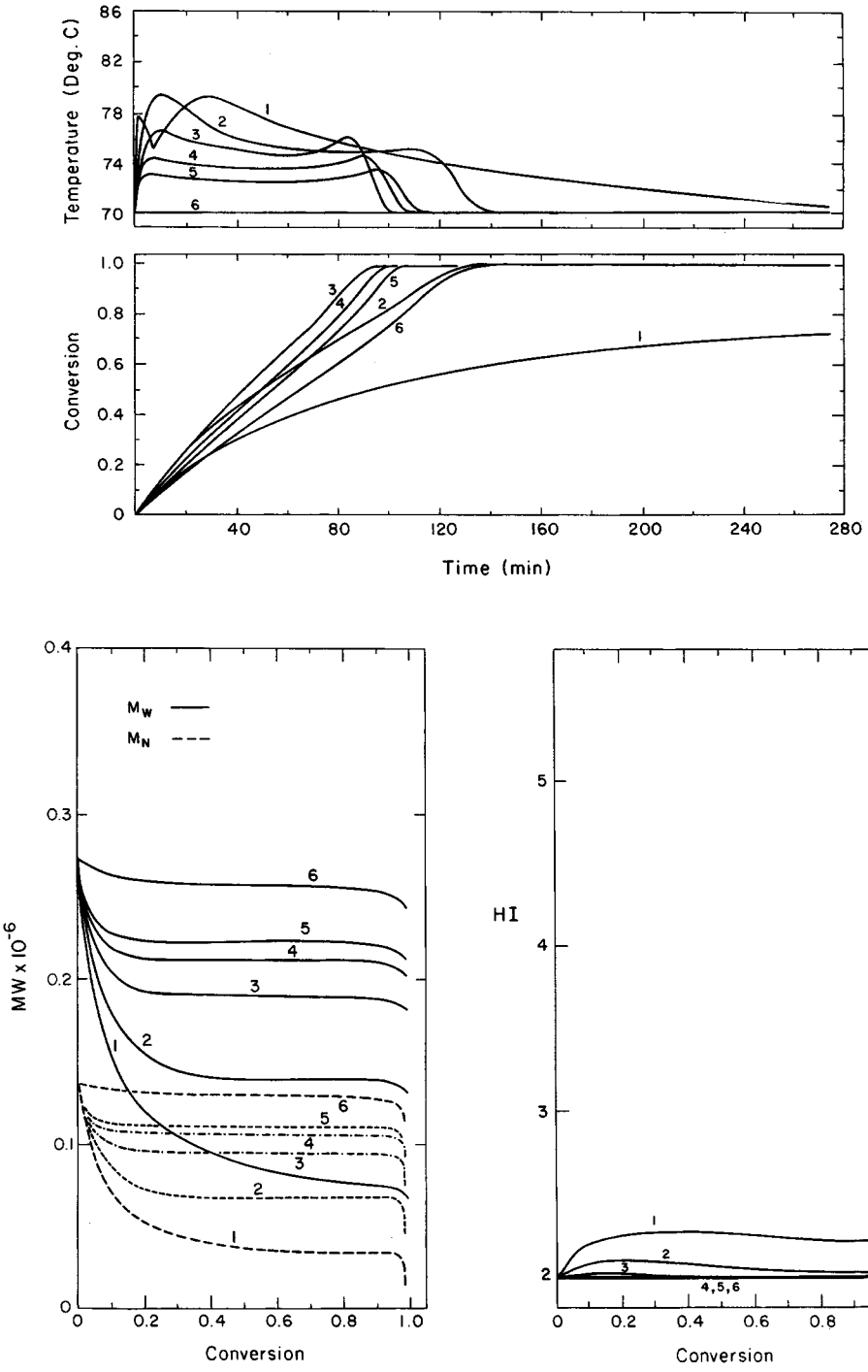

Fig. 16. Model predictions for optimum (minimum HI) nonisothermal solvent addition with solvent cooling. $T_s = T_f = 70°C$; $I_0 = 0.0258M$ AIBN; $V_0 = 0.5$ L; $A = 486.3$ cm^2. Multiply U (Btu/h ft^2 °F) by 4.88 to convert to U (kcal/h m^2 °C). U (Btu/h ft^2 °F): (1) 10; (2) 20; (3) 30; (4) 40; (5) 50; (6) ∞.

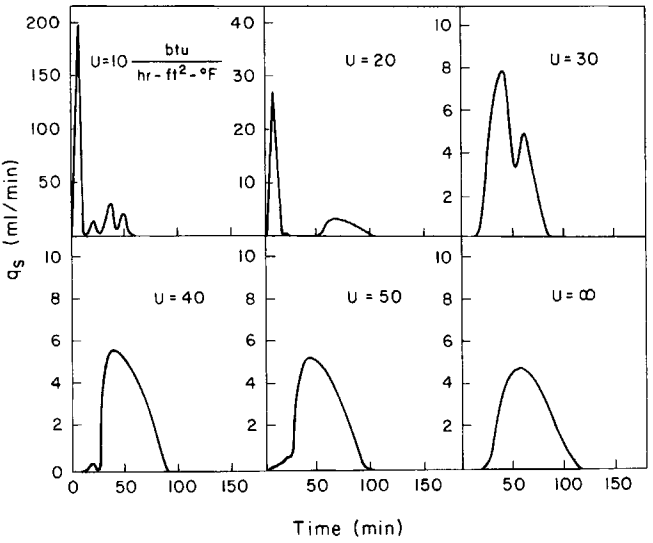

Fig. 17. Variation of the optimum nonisothermal solvent addition profile with solvent cooling. Notice the decrease in the quantity of solvent delivered as isothermal conditions are reached.

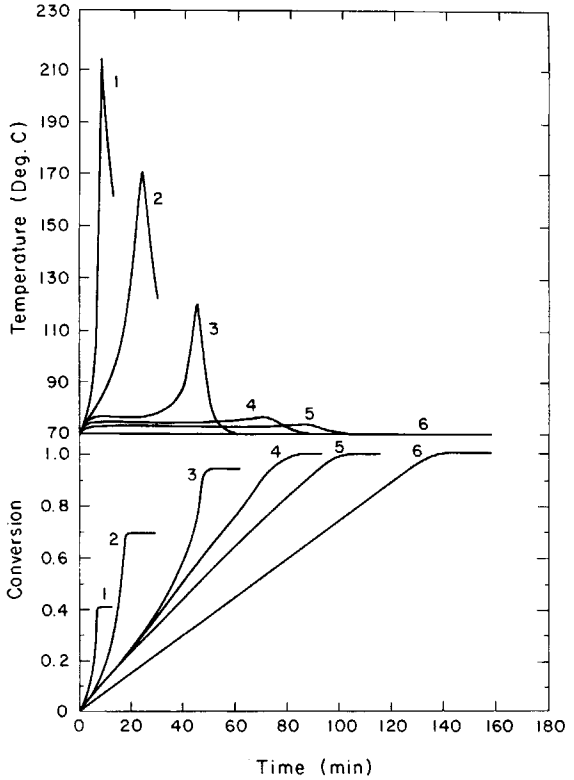

Fig. 18. Optimum nonisothermal solvent addition without solvent cooling. T_s = 70°C; I_0 = 0.0258M AIBN; V_0 = 0.5 L; A = 486.3 cm². Much higher temperatures are encountered than cases with solvent cooling, but less solvent is needed. U (Btu/h ft² °F): (1) 10; (2) 20; (3) 30; (4) 40; (5) 50; (6) ∞.

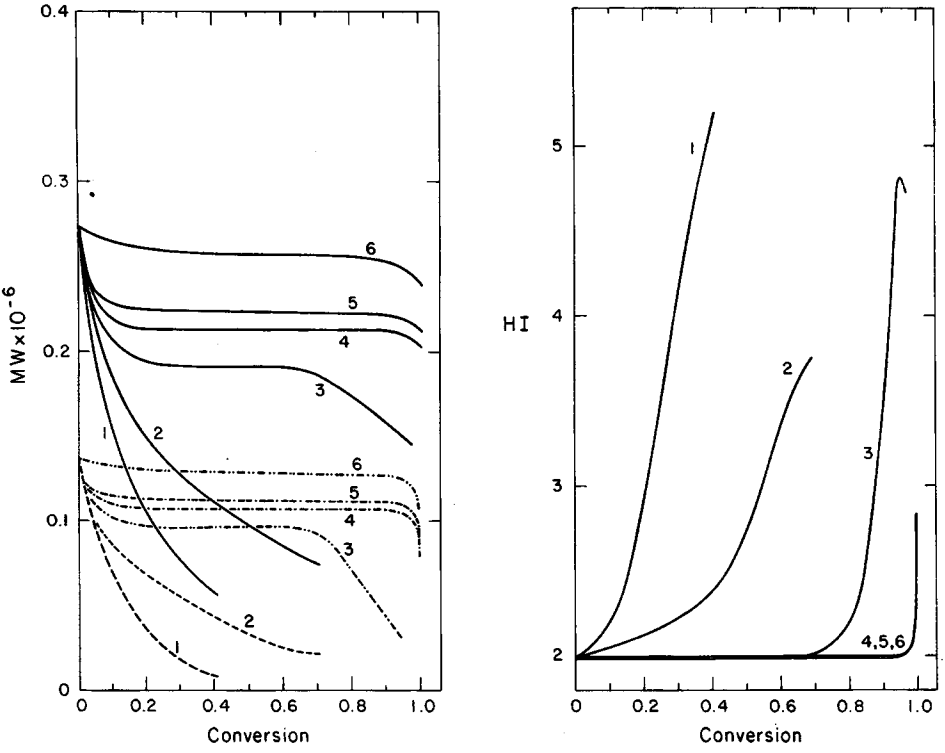

Fig. 19. The effect of heat transfer coefficient on the molecular weight and polydispersity produced by the optimum nonisothermal solvent addition without solvent cooling. The same conditions are used as in Figure 18. Left: (—) M_w; (- - -) M_n. U (Btu/h ft² °F): (1) 10; (2) 20; (3) 30; (4) 40; (5) 50; (6) 60.

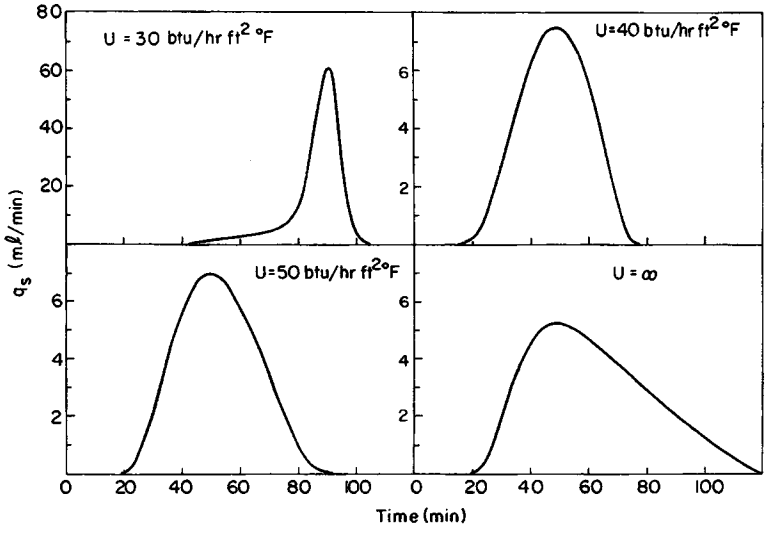

Fig. 20. Variation of the optimum nonisothermal solvent addition profile without solvent cooling. No solvent is needed at U = 10 and 20 Btu/h ft² °F as the reaction dead ends before the gel effect occurs.

(as governed by the overall heat transfer coefficient) is much greater than the rate of heat generation. Shorter batch times are obtained as the reaction temperature rises. However, when near-adiabatic heat transfer conditions are reached, large quantities of solvent must be added to cool the reactor and to prevent thermal runaway. This decreases the rate of propagation and much longer batch times are needed to reach a given conversion under these conditions. Hence, the batch time first decreases then increases again with decreasing heat transfer efficiency.

At large heat transfer rates, reaction temperature rises rapidly until the rate of heat generation matches that of heat removal. Temperature then remains constant until the reaction nears completion whereupon the temperature drops off. At low heat transfer rates, solvent addition (added at the initial temperature) provides extra cooling. It also dilutes the reactants while increasing the overall heat capacity of the reacting mixture. Reactor temperature continues to rise until the solvent has lowered the rate of propagation to the point where heat removal is again equal to heat generation. The temperature then falls off slowly for the rest of the reaction.

MW decreases until either the steady-state temperature is reached or reaction temperature begins to fall. Final product MWs will be lower than those produced under isothermal conditions due to the higher rates of initiation and termination. PD is minimized at high heat transfer rates. At low heat transfer rates, PD increases until the temperature can be brought under control. Thereafter, PD drops slightly with decreasing temperature. PD eventually rises in all cases as complete conversion is approached.

The amount of solvent added increases with decreasing heat transfer rate. Near-isothermal conditions are strictly required to minimize the quantity of solvent used per batch. Solvent addition profiles are dominated by huge sharp solvent peaks at low heat transfer rates. Very little additional solvent is needed to control the gel effect since the reaction temperature is usually high and copious amounts of solvent already exist at that point. As heat transfer rates increase, the cooling peak decreases and merges with the gel effect peak. Under near-isothermal conditions, only the gel effect solvent peak remains.

Figures 18–20 show the optimum nonisothermal behavior when the solvent is added at the existing reactor temperature. No solvent is required at near-adiabatic conditions as the polymerization dead-ends. Under these conditions, the MWD would greatly broaden via chain transfer reactions. Minimal quantities of solvent are needed when thermal ignition occurs. Here, high temperature and chain transfer both help to maintain the instantaneous MW constant. However, PD still increases from the greatly facilitated chain transfer at high temperatures. Larger amounts of solvent must be added under near-isothermal conditions when the temperature excursions are not as great. Only at these conditions are low PDs obtained.

Since near-isothermal conditions are more desirable, high rates of heat transfer are important. In designing a new reactor, this is achieved by selecting the appropriate structural materials to give the desired overall heat transfer coefficient. For existing reactors, the heat transfer coefficient is largely fixed (U also depends on agitation). However, heat transfer can be dramatically improved by operating at low pressures with a reflux con-

denser. Additional cooling may also be obtained by lowering the solvent feed temperature or by dropping the surrounding cooling water temperature in a jacketed vessel. These alternatives are investigated below.

When the solvent is added at a temperature lower than the initial reactor temperature, the polymerization is quenched (see Figs. 21–23). Reactor temperature declines due to solvent cooling and the increased heat capacity of the solution and the lowered rate of heat generation. Lower temperatures lead to lower rates of initiation and termination. Radical lifetimes are extended and MWs would increase if the system were left uncontrolled. However, the optimum profile continuously adds solvent to promote chain transfer. This minimizes PD, but both cumulative weight and number average MW decrease. When temperature levels off, a new radical population with a vastly lowered average chain length is formed. A bimodal MWD then results. PD increases rapidly as soon as the temperature levels off. Only when solvent feed temperatures approximate surrounding temperatures does the reaction temperature rise again and any significant polymerization resumes. However, PD continues to increase and both MW averages full until the temperature levels off.

When the surrounding temperature is below the initial reactor temperature, the polymerization is again quenched (See Figs. 24–26). Low conversions are obtained as reaction rates are slowed by the declining temperature. Reactor temperature decreases until it reaches the surrounding temperature. If left uncontrolled, polymers of increasing length would be produced and the MWD skewed. However, solvent addition limits the chain length by chain transfer. Both number and weight average MWs can be held constant. PD increases initially when the weight average MW shifts

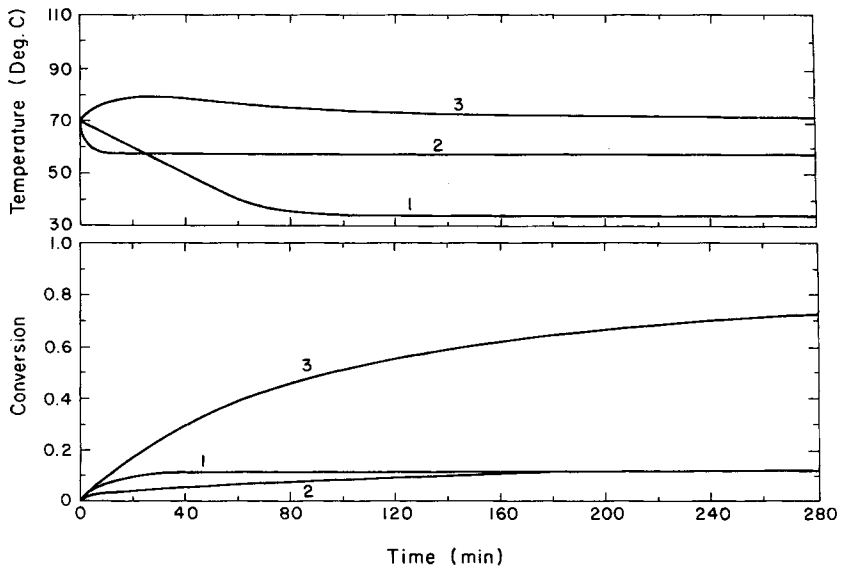

Fig. 21. Influence of the solvent feed temperature on the optimum nonisothermal solvent addition policy. Solvent apparently is added for its heating or cooling value. T = 70°C; I_0 = 0.0258M AIBN; U = 10 Btu/h ft² °F; V_0 = 0.5L; A = 486.3 cm²; T_{sf} (°C): (1) 25; (2) 50; (3) 70.

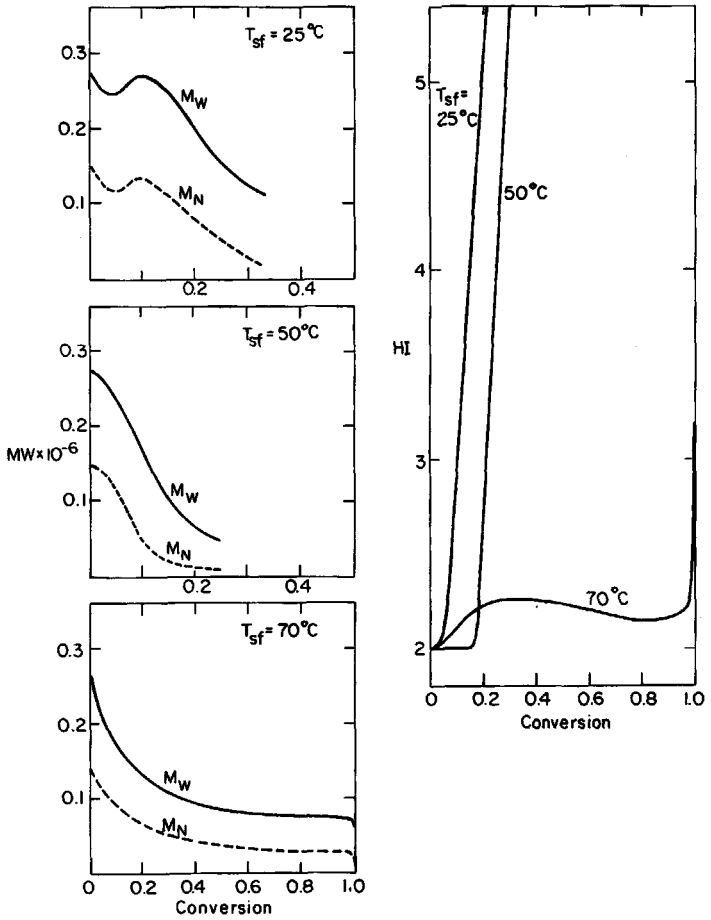

Fig. 22. The effect of solvent feed temperature on the molecular weight and polydispersity produced by the optimum nonisothermal solvent addition. The same conditions apply as in Figure 21.

upward due to the decreased termination rates. PD decreases when the surrounding temperature is reached as $\overline{M}_n$ rises relative to $\overline{M}_w$.

If the surrounding temperature is above the initial reactor temperature, solvent will be added to cool the reactor and stabilize the temperature. Higher conversions are reached, since the reaction rates are faster at higher temperatures. MWs fall because of the faster initiation and chain transfer rates. PD increases from the start of the reaction since $\overline{M}_n$ falls faster than $\overline{M}_w$. Solvent cooling is continuously needed as heat enters from the warmer surroundings. This floods the reactor and stops the polymerization via dilution of both monomer and initiator.

The highest conversion is produced when the initial temperature is equal to the surrounding cooling medium temperature. Reactor temperature again rises as the initial rate of heat generation exceeds the rate of heat transfer. But once solvent cooling has begun, the reaction rate slows down and the rate of heat generation drops correspondingly. Temperature con-

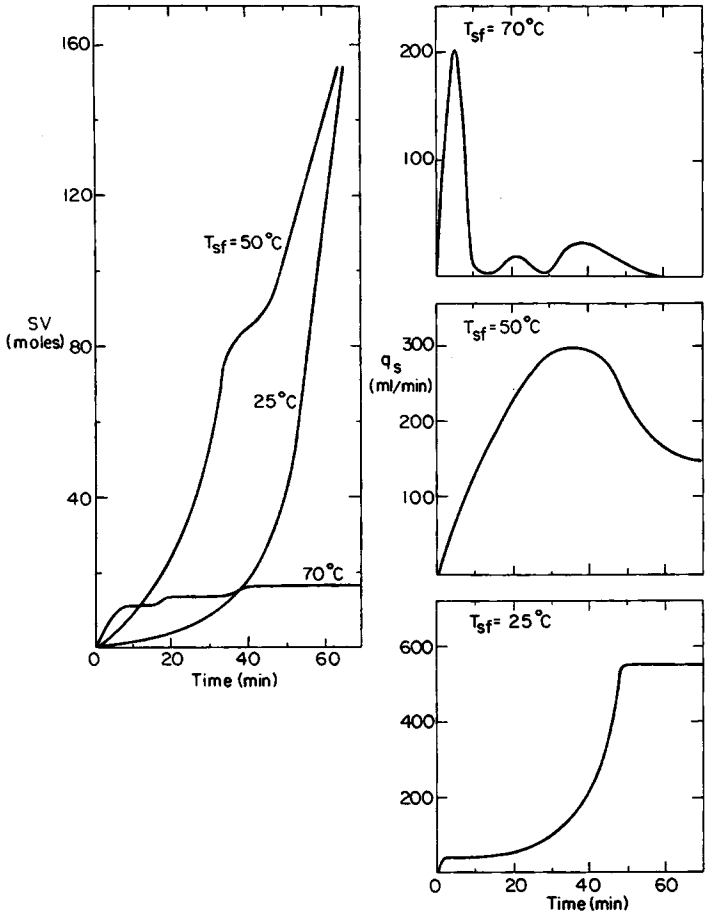

Fig. 23. Comparison of the optimum nonisothermal solvent addition profiles for different feed temperatures for conditions given in Figure 21.

tinues to fall when the cooling capacity surpasses the heat generated. This minimizes the amount of additional solvent needed. The reaction is not quenched totally and high conversions can eventually be reached. $\overline{M}_n$ falls faster than $\overline{M}_w$ as temperature first rises, but again increases quickly when temperature drops. $\overline{M}_n$ eventually drops due to concentration drift from monomer depletion at very high conversions. These phenomena cause the overall PD to undergo a local maximum and minimum.

Comments on Optimal Strategies

The optimum temperature, initiation, and monomer and solvent addition histories have been compared with the reference batch case in Figures 2, 7, 9, and 10. All optimal strategies except for monomer addition achieve high conversion. Both temperture and nonisothermal photoinitiation control lead to shorter batch times, while solvent addition requires slightly longer cycle times. Most policies maintain a constant or near-constant num-

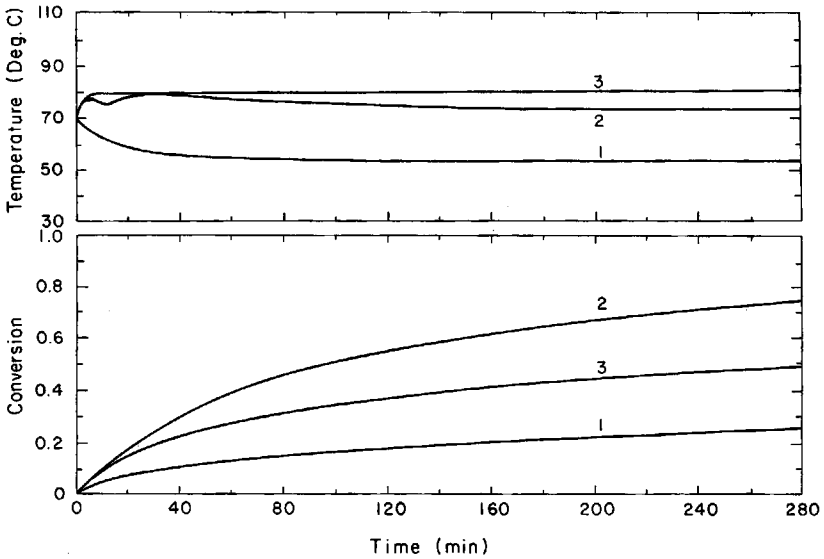

Fig. 24. Influence of the surrounding temperature on the optimum nonisothermal solvent addition policy. Solvent apparently is added for its heating or cooling value until isothermal conditions are reached. T = 70°C; I_0 = 0.0258M AIBN; U = 10 Btu/h ft² °F; V_0 = 0.5L; A = 486.3 cm²; T_s (°C): (1) 50; (2) 70; (3) 90.

ber and weight MW throughout most of the polymerization. All policies lead to a significant reduction in PD when compared with that obtained in an uncontrolled batch run. However, not all optimum policies are equal.

Monomer addition is a viable control strategy when both gel and glass effects are absent. However, for MMA, this control method suffers from low conversion, and so large quantities of monomer must be recycled per batch. High reaction temperatures are favored, but then only relatively low MW polymers are produced. A pure product with only trace amounts of residual initiator is obtained. Monomer addition is only a realistic improvement when (1) the semibatch reactor is used as a prepolymerizer or (2) monomer addition is used in conjunction with selective solvent addition, or programmed temperature or photoinitiation to eliminate the gel effect. Monomer addition is favored over a conventional batch prepolymerizer because efficient usage of initiators is achieved. Still, of the different control schemes, it is deemed the least practical.

Temperature control enjoys the advantage of being able to generate a pure product. A major disadvantage of the method is that rapid temperature changes are required in a short span of time. These variations are difficult to enforce in practice. Heat transfer through the polymerizing medium is hampered by the high viscosity and poor thermal conductivity of the polymer. Uniform mixing is difficult at high conversions, and so local hot spots may occur. Complete conversion is not desired unless the resulting polymer is melt extruded. A glass is generally formed in the reactor.

Photoinitiation control is practical since it allows for rapid changes in initiation. Pure PMMA is also obtained with this method. Glass formation

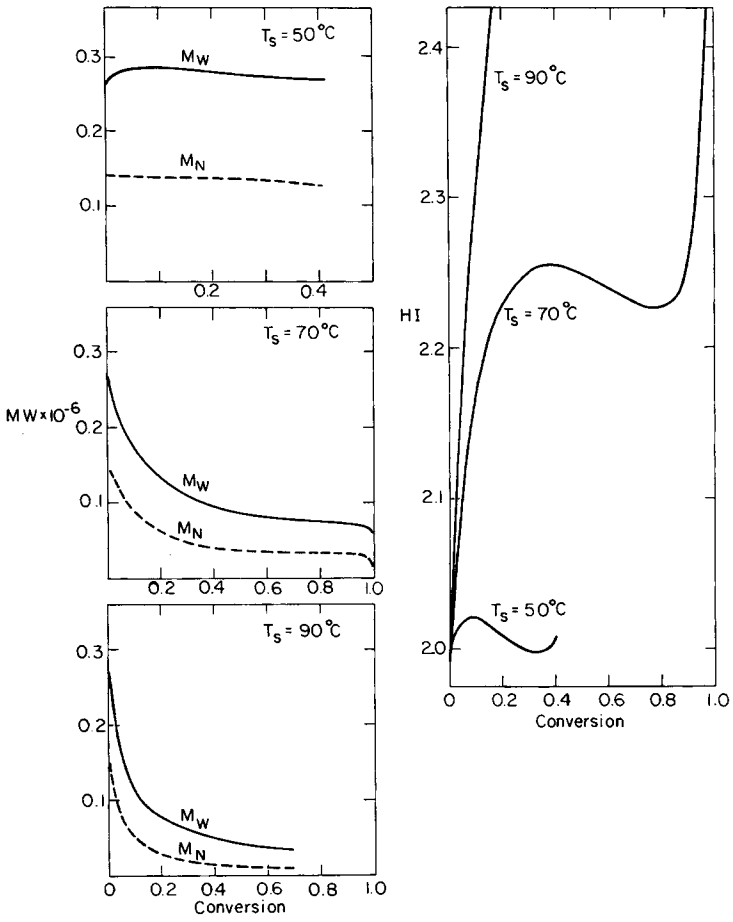

Fig. 25. Effects of the surrounding temperature on the molecular weight and polydispersity produced by the optimum nonisothermal solvent addition for the conditions given in Figure 24.

must be avoided to prevent reactor plugging. The high viscosity is not a problem as initiation is independent of temperature. Since PMMA is transparent, spatially uniform initiation is easily attained. Heat transfer is not a limitation as nonisothermal situations are actually favored over isothermal conditions. The method is thus easier to execute than temperature control.

Solvent addition is by far the easiest to carry out in practice. Complete conversion can be obtained with slightly longer batch times than the ordinary isothermal reference case. Addition of a solvent lowers the viscosity and enhances mixing. Solvent also improves both the heat capacity and heat transfer properties. Isothermal conditions are preferred over nonisothermal conditions. The only real disadvantage of the method is that a solvent separation step is needed to obtain the pure polymer. Discoloration and deterioration of optical properties can be minimized by using transparent, stable solvents.

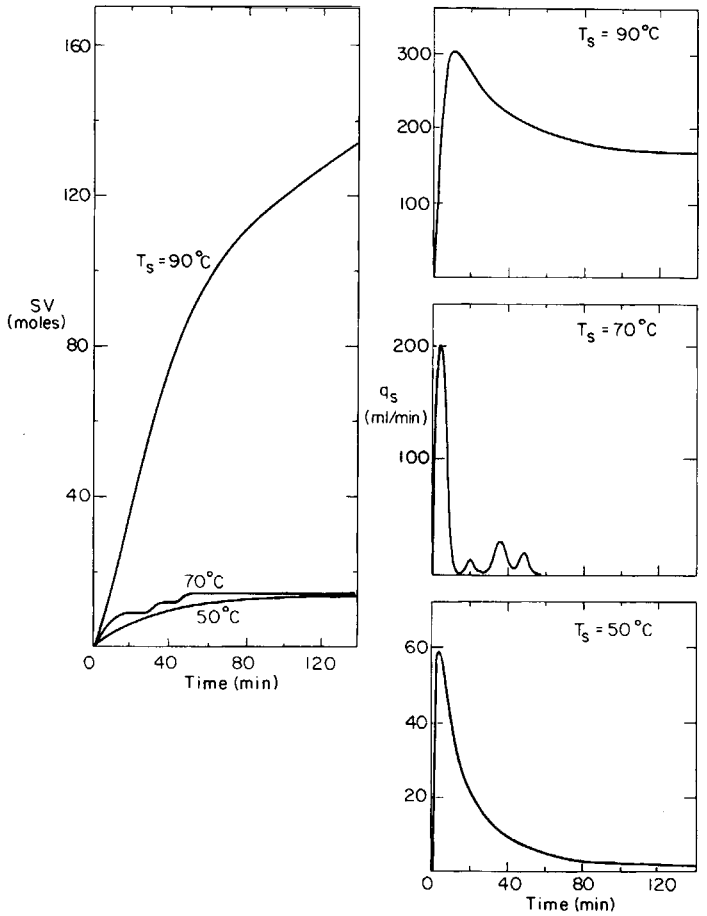

Fig. 26. Comparison of the optimum nonisothermal solvent addition profiles for different surrounding temperatures. Conditions are the same as in Figure 24.

References

1. J. R. Martin, J. F. Johnson, and A. R. Cooper, *J. Macromol. Sci. Rev. Macromol. Chem.*, **C8**, 57 (1972).

2. J. R. Martin, R. W. Nunes, and J. F. Johnson, *Polym. Eng. Sci.*, **22**, 205 (1982).

3. K. Osakada and L. T. Fan, *J. Appl. Polym. Sci.*, **14**, 3065 (1970).

4. R. A. Aris, *The Optimal Design of Chemical Reactors*, Academic, New York, 1961.

5. C. G. Hill, Jr., *Introduction to Chemical Engineering Kinetics and Reactor Design*, Wiley, New York, 1977.

6. G. F. Froment and K. B. Bischoff, *Chemical Reactor Analysis and Design*, Wiley-Interscience, New York, 1979.

7. R. F. Hoffman, S. Schreiber, and G. Rosen, *Ind. Eng. Chem.*, **56**, 51 (1964).

8. J. A. Biesenberger and Z. Tadmor, *Polym. Lett.*, **3**, 753 (1965).

9. Z. Tadmor and J. A. Biesenberger, *IEC Fundamentals*, **5**, 336 (1966).

10. K. G. Denbigh, *J. Appl. Chem.*, **1**, 227 (1951).

11. H. Nishimura and F. Yokoyama, *Kagaku Kogaku*, **32**, 601 (1968).

12. J. Hicks, A. Mohan, and W. H. Ray, *Can. J. Chem. Eng.*, **47**, 590 (1969).

13. M. E. Sachs, S. Lee, and J. A. Biesenberger, *Chem. Eng. Sci.*, **28**, 241 (1973).

14. P. E. King and J. M. Skaates, *Ind. Eng. Chem., Proc. Des. Dev.*, **8**, 114 (1969).

15. Y. Yoshimoto, H. Yanagawa, T. Suzuki, T. Araki, and Y. Inaba, *Kagaku Kogaku,* **132**, 595 (1968).
16. Y. Yoshimoto, H. Yanagawa, T. Suzuki, T. Araki, and Y. Inaba, *Int. Chem. Eng.,* **11**, 147 (1971).
17. G. Z. A. Wu, L. A. Denton, and R. L. Laurence, *Polym. Eng. Sci.,* **22**, 1 (1982).
18. M. E. Sachs, S. Lee, and J. A. Biesenberger, *Chem. Eng. Sci.,* **27**, 2281 (1972).
19. S. Chen and W. Jeng, *Chem. Eng. Sci.,* **33**, 735 (1978).
20. S. Chen and N. Huang, *Chem. Eng. Sci.,* **36**, 1295 (1981).
21. M. M. Denn, *Optimization by Variational Methods,* Krieger, Huntington NY, 1978.
22. W. Y. Chiu, G. M. Carratt, and D. S. Soong, *Macromolecules,* **16**, 348 (1983).
23. B. M. Louie and D. S. Soong, *J. Polym. Sci.,* to appear.
24. H. T. Chen, C. N. Kuan, and D. J. Lin, *AIChE J.,* **28**, 214 (1982).
25. T. G. Gutowski, N. P. Suh, C. Cangialose, and G. M. Berube, *Polym. Sci. Eng.,* **23**, 230 (1983).
26. S. Carra, M. Morbidelli, E. Santacesaria, and G. Niederjaufner, *J. Appl. Polym. Sci.,* **26**, 1497 (1981).
27. G. V. Schultz and G. Harborth, *Macromol. Chem.,* **1**, 106 (1947).
28. K. Ito, *J. Polym. Sci., Polym. Chem. Ed.,* **13**, 401 (1975).

Received September 20, 1984
Accepted January 11, 1985